

Synthesis, Characterization, and Optical Properties of Pentafluorophenyl Complexes with a Pt–Cd Bond

Juan Forniés,* Susana Ibáñez, and Antonio Martín

Departamento de Química Inorgánica, Instituto de Ciencia de Materiales de Aragón, Universidad de Zaragoza, CSIC, 50009 Zaragoza, Spain

Belén Gil, Elena Lalinde,* and M. Teresa Moreno

Departamento de Química, Grupo de Síntesis Química de La Rioja, UA, CSIC, Universidad de La Rioja, 26006, Logroño, Spain

Received April 19, 2004

Novel bimetallic neutral $[(C_6F_5)_4PtCd(cyclen)]$ and $[(C_6F_5)_2(C\equiv CPh)_2PtCd(cyclen)]$ (**1**, **2**) and cationic $[(C_6F_5)_2(bzq)PtCd(cyclen)](ClO_4)$ (**3**) pentafluorophenylplatinum(II)–cadmium(II) derivatives have been prepared by treatment of the adequate anionic starting precursors $[Pt(C_6F_5)_2X_2]^{n-}$ ($n = 2$, $X = C_6F_5$, $C\equiv CPh$; $n = 1$, $X_2 = bzq$) with $Cd(ClO_4)_2$ and cyclen. X-ray diffraction studies on complexes **1**, **2**, and **3** show that they are stabilized by a short Pt→Cd donor acceptor bond and, additionally, in complex **2** the Cd center is also coordinated to the C_α of one of the two alkynyl groups. In contrast, treatment of the binuclear compound $[NBu_4]_2[Pt_2(\mu-Cl)_2(C_6F_5)_4]$ with $[Cd(cyclen)(MeOH)_2](ClO_4)_2$ afforded the tetranuclear derivative $[Pt(C_6F_5)_2Cl(\mu-Cl)Cd(cyclen)]_2$ (**4**) (X-ray), in which Pt and Cd atoms are connected by a μ_3 -Cl bridging ligand, and the binuclear cadmium complex $[Cd_2(\mu-Cl)_2(cyclen)_2](ClO_4)_2$ (**5**) (X-ray), in which two “Cd(cyclen)” fragments are bridged by two chlorine atoms. The photoluminescent properties of complexes **1–3** have also been examined and compared with those of their corresponding anionic parent compounds $[NBu_4]_2[Pt(C_6F_5)_4]$, $[PMePh_3]_2[Pt(C_6F_5)_2(C\equiv CPh)_2]$, and $[NBu_4][Pt(C_6F_5)_2(bzq)]$ (**6**).

Introduction

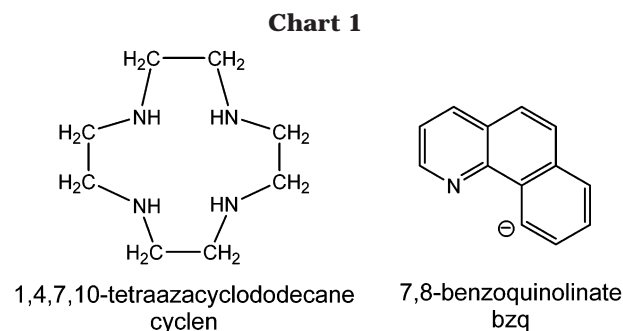
Although several heteropolymetallic systems involving Pt(II) and Cd(II) have been reported,¹ in most of them the metal centers are connected by bridging ligands and, as far as we know, Pt(II)–Cd(II) interactions have been structurally characterized only in a few cases. Our recent interest in heteropolynuclear alkynyl complexes² based on $Pt\cdots M$ and $M\cdots acetylenic$ interactions led us to the isolation of two of them: $[NBu_4]_2[Pt(\mu-\kappa C^{\alpha}C^{\alpha}-C\equiv CPh)_2(CdCl)_2]$ ³ and $[Pt_4Cd_6(C\equiv CPh)_4(\mu-C\equiv CPh)_{12}(\mu_3-OH)_4]$,⁴ which have been prepared by the reaction of $[NBu_4]_2[Pt(C\equiv CPh)_4]$ with $CdCl_2$ or $Cd(ClO_4)_2 \cdot 6H_2O$, respectively. Both complexes are lumi-

(1) (a) Pettinari, C.; Marchetti, F.; Cingolani, A.; Troyanov, S. I.; Drozdov, A. *J. Chem. Soc., Dalton Trans.* **1998**, 3335. (b) Li, Z.; Zheng, W.; Liu, H.; Mok, K. F.; Hor, T. S. A. *Inorg. Chem.* **2003**, *42*, 8481. (c) Capdevila, M.; Carrasco, Y.; Clegg, W.; Coxall, R. A.; González-Duarte, P.; Lledós, A.; Ramírez, J. A. *J. Chem. Soc., Dalton Trans.* **1999**, 3103. (d) Li, Z.; Loh, Z.-H.; Audi Fong, S.-W.; Yan, Y.-K.; Henderson, W.; Mok, K. F.; Andy Hor, T. S. *J. Chem. Soc., Dalton Trans.* **2000**, 1027.

(2) (a) Chartmant, J. P. H.; Forniés, J.; Gómez, J.; Lalinde, E.; Merino, R. I.; Moreno, M. T.; Orpen, A. G. *Organometallics* **2003**, *22*, 652. (b) Ara, I.; Berenguer, J. R.; Eguizabal, E.; Forniés, J.; Gómez, J.; Lalinde, E. *J. Organomet. Chem.* **2003**, *670*, 221. (c) Berenguer, J.; Forniés, J.; Gómez, J.; Lalinde, E.; Moreno, M. T. *Organometallics* **2001**, *20*, 4847. (d) Ara, I.; Forniés, J.; Gómez, J.; Lalinde, E.; Moreno, M. T. *Organometallics* **2000**, *19*, 3137. (e) Chartmant, J. P. H.; Forniés, J.; Gómez, J.; Lalinde, E.; Merino, R. I.; Moreno, M. T.; Orpen, G. A. *Organometallics* **1999**, *18*, 3353. (f) Ara, I.; Berenguer, J. R.; Forniés, J.; Gómez, J.; Lalinde, E.; Merino, R. I. *Inorg. Chem.* **1997**, *36*, 6461.

(3) Chartmant, J. P. H.; Falvello, L. R.; Forniés, J.; Gómez, J.; Lalinde, E.; Moreno, M. T.; Orpen, A. G.; Rueda, A. *Chem. Commun.* **1999**, 2045.

(4) Forniés, J.; Gómez, J.; Lalinde, E.; Moreno, M. T. *Inorg. Chem.* **2001**, *40*, 5415.



nescent and display weak Pt–Cd bonding interactions (2.960(1) and 2.857(1) Å) and Cd–acetylide bonds, the latter probably being the driving force for the formation of these complexes. The other complexes $\{[(phpy)_2PtCd(cyclen)](ClO_4)_2$ and $[(bpy)Me_2PtCd(cyclen)](ClO_4)_2$ (Hphpy = 2-phenylpyridine, bpy = 2,2'-bipyridine, cyclen = 1,4,7,10-tetraazacyclododecane, see Chart 1)} have been prepared by Ito et al.⁵ by reacting the corresponding platinum precursors with $[Cd(cyclen)(MeOH)_2](ClO_4)_2$, the Pt→Cd bonds being very short (2.639(1) and 2.610(1) Å, respectively) and totally unsupported by any kind of bridging interaction between the two metal centers.

In the course of our current research on pentahalophenyl platinate complexes with Pt→M (M =

(5) Yamaguchi, T.; Yamazaki, F.; Ito, T. *J. Am. Chem. Soc.* **1999**, *121*, 7405

Ag(I), Tl(II), Pb(II), Sn(II) donor–acceptor bonds⁶ we have prepared complexes with structures similar to the ones displayed by Ito's complexes, although in our case, the pentafluorophenyl groups are specially oriented so as to form $\sigma\text{-F}\cdots\text{M}$ secondary interactions, which had been considered as an additional factor for stabilizing the Pt→M donor–acceptor bonds.⁶

We thought it would be interesting to explore the reactions of the pentahalophenyl platinum(II) anionic complexes with a simple cadmium salt ($\text{Cd}(\text{ClO}_4)_2$) and with “ $\text{Cd}(\text{cyclen})^{2+}$ ” in order to see how important the negative charge of the anionic complex and the presence of the C_6X_5 ligand is in the formation of the complexes. We are now reporting the results of these reactions, which allow the preparation of novel bimetallic neutral $[(\text{C}_6\text{F}_5)_4\text{PtCd}(\text{cyclen})]$ and $[(\text{C}_6\text{F}_5)_2(\text{C}\equiv\text{CPh})_2\text{PtCd}(\text{cyclen})]$ (**1**, **2**) and cationic $[(\text{C}_6\text{F}_5)_2(\text{bzq})\text{PtCd}(\text{cyclen})](\text{ClO}_4)$ (**3**) ($\text{bzq} = 7, 8\text{-benzoquinoline}$, see Chart 1) systems containing Pt–Cd bonding interactions and also a tetranuclear Pt_2Cd_2 (**4**) derivative in which Pt and Cd atoms are connected by a $\mu_3\text{-Cl}$ bridging ligand.

One important property of some mixed-metal systems containing closed-shell metal \cdots metal contacts, including $d^8\text{--}d^8$ and $d^8\text{--}d^{10}$ metal complexes or aggregates, is that they are often intensely luminescent, making them attractive with respect to potential applications.⁷ In fact, the nature and the role of metallophilic bonding interactions in the photophysical properties of this type of system are currently an area of intense research.^{2,8} In an effort to provide further insight into the importance of the $d^8\cdots\text{M}$ bonding interactions in the nature of the excited-state origin of these complexes, the optical properties of complexes **1–3** have also been examined.

Results and Discussion

Reaction of $[\text{NBu}_4]_2[\text{Pt}(\text{C}_6\text{F}_5)_4]$ with $\text{Cd}(\text{ClO}_4)_2$.

The reaction of the perhaloaryl anionic complex $[\text{NBu}_4]_2[\text{Pt}(\text{C}_6\text{F}_5)_4]$ toward the simple cadmium salt $\text{Cd}(\text{ClO}_4)_2$ in dichloromethane and in 1:1 or 1:2 molar ratio has been investigated. In all cases unreacted platinum starting material is recovered, along with a solid that is a mixture of compounds which we have not been able to separate but whose ¹⁹F NMR spectrum indicates the presence of $[\text{Pt}_2(\mu\text{-C}_6\text{F}_5)_2(\text{C}_6\text{F}_5)_4]^{2-}$, previously synthe-

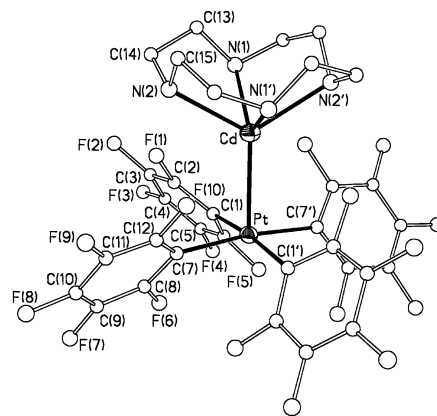


Figure 1. Structure of the complex $[(\text{C}_6\text{F}_5)_4\text{PtCd}(\text{cyclen})]$ (**1**).

sized and characterized in our group,⁹ and which contains bridging pentafluorophenyl groups. This seems to indicate that, at least partially, the naked Cd(II) center acts as a dearyllating agent toward the platinum in $[\text{Pt}(\text{C}_6\text{F}_5)_4]^{2-}$.

Synthesis and Structural Characterization of Neutral $[(\text{C}_6\text{F}_5)_4\text{PtCd}(\text{cyclen})]$ (1**) and $[(\text{C}_6\text{F}_5)_2(\text{C}\equiv\text{CPh})_2\text{PtCd}(\text{cyclen})]$ (**2**).** The reactions of several Pt complexes toward “ $\text{Cd}(\text{cyclen})^{2+}$ ”, which has proved to be so useful for preparing complexes containing unsupported Pt→Cd bonds,⁵ result in the formation of Pt–Cd derivatives. Thus, when $[\text{NBu}_4]_2[\text{Pt}(\text{C}_6\text{F}_5)_4]$ is added to a solution of $[\text{Cd}(\text{cyclen})(\text{MeOH})_2](\text{ClO}_4)_2$ in MeOH prepared “in situ” (see Experimental Section and Scheme 1i), in 1:1 molar ratio, the precipitation of a white solid is observed upon stirring at room temperature for a few minutes. This white solid is separated by filtration and identified as $[(\text{C}_6\text{F}_5)_4\text{PtCd}(\text{cyclen})]$ (**1**).

A single-crystal X-ray diffraction study of **1** has been carried out, and its structure is shown in Figure 1. Crystallographic data are given in Table 1, and selected interatomic distances and angles appear in Table 2. **1** is a dinuclear complex formed by the moieties “ $\text{Pt}(\text{C}_6\text{F}_5)_4$ ” and “ $\text{Cd}(\text{cyclen})$ ” bonded through a Pt–Cd bond. The environment of the platinum atom is square planar. The Pt–C distances are the usual ones for this kind of complex.¹⁰ The platinum atom lies in the center of the square in such a way that it separates slightly (0.136(1) Å) from the best plane formed by the four C_{ipso} atoms toward the Cd atom. The geometry of the “ $\text{Cd}(\text{cyclen})$ ” fragment is similar to that found in other complexes containing it.⁵

The platinum and cadmium atoms are linked by a bond that is unsupported by any covalent bridging ligand. The Pt–Cd distance is 2.775(1) Å, which is

(6) Forniés, J.; Martín, A. In *Metal Clusters in Chemistry*; Braunschweig, P., Oro, L. A., Raithby, P. R., Eds.; Wiley-VCH: Weinheim, 1999; Vol. 1, pp 417–443.

(7) For some reviews see: (a) Gliemann, G.; Yersin, H. *Struct. Bonding* **1985**, *62*, 87. (b) Rhoadhill, D. M.; Gray, H. B.; Che, C. M. *Acc. Chem. Res.* **1989**, *22*, 55. (c) Forward, J. M.; Fackler, J. P., Jr.; Assefa, Z. In *Optoelectronic Properties of Inorganic Compounds*; Plenum: New York, 1999; p 195. (d) Fung, E. Y.; Olmstead, M. M.; Vickery, J. C.; Balch, A. L. *Coord. Chem. Rev.* **1998**, *171*, 151. (e) Gade, L. H. *Angew. Chem., Int. Ed. Engl.* **1997**, *36*, 1171; **2001**, *40*, 3573. (f) Pyykkö, P. *Chem. Rev.* **1997**, *97*, 597.

(8) For some recent examples see: (a) Coker, N. L.; Bauer, J. A. K.; Elder, R. C. *J. Am. Chem. Soc.* **2004**, *126*, 12. (b) Stender, M.; Olmstead, M. M.; Balch, A. L.; Rios, D.; Attar, S. *Dalton Trans.* **2003**, 4282. (c) Jalilvand, F.; Eriksson, L.; Glaser, J.; Malirik, M.; Mink, J.; Sandström, M.; Tóth, I.; Tóth, J. *Chem. Eur. J.* **2001**, *7*, 2167. (d) Cariati, E.; Bu, X.; Ford, P. C. *Chem. Mater.* **2000**, *12*, 3385. (e) Fernández, E. J.; López de Luzuriaga, J. M.; Monge, M.; Olmos, M. E.; Pérez, J.; Laguna, A. *J. Am. Chem. Soc.* **2002**, *124*, 5942. (f) Catalano, V. J.; Bennett, B. L.; Kar, H. M.; Noll, B. C. *J. Am. Chem. Soc.* **1999**, *121*, 10235. (g) Rawashdeh-Omary, M. A.; Omary, M. A.; Patterson, H. H.; Fackler, J. P., Jr. *J. Am. Chem. Soc.* **2001**, *123*, 11237. (h) Lee, Y. A.; McGarrah, J. E.; Lachicotte, R. J.; Eisenberg, R. J. *J. Am. Chem. Soc.* **2002**, *124*, 10662. (i) Omari, M. A.; Webb, T. R.; Assefa, Z.; Shankle, G. E.; Patterson, H. H. *Inorg. Chem.* **1998**, *37*, 1380. (j) Yam, W. W. V.; Hui, C. K.; Yu, S. Y.; Zhu, N. *Inorg. Chem.* **2004**, *43*, 812.

(9) Usón, R.; Forniés, J.; Tomás, M.; Casas, J. M.; Cotton, F. A.; Falvello, L. R.; Llusar, R. *Organometallics* **1988**, *7*, 2279.

(10) See for example: (a) Cotton, F. A.; Falvello, L. R.; Usón, R.; Forniés, J.; Tomás, M.; Casas, J. M.; Ara, I. *Inorg. Chem.* **1987**, *26*, 1366. (b) Bellamy, D.; Connely, N. G.; Lewis, G. R.; Orpen, A. G. *Cryst. Eng. Commun.* **2002**, *4*, 68. (c) Casas, J. M.; Forniés, J.; Martínez, F.; Rueda, A. J.; Tomás, M.; Welch, A. J. *Inorg. Chem.* **1999**, *38*, 1529. (d) Usón, R.; Forniés, J.; Tomás, M.; Ara, I. *J. Chem. Soc., Dalton Trans.* **1989**, 1011. (e) Usón, R.; Forniés, J.; Tomás, M.; Martínez, F.; Casas, J. M.; Fortuño, C. *Inorg. Chim. Acta* **1995**, *235*, 51. (f) Usón, R.; Forniés, J.; Tomás, M.; Ara, I.; Casas, J. M.; Martín, A. *J. Chem. Soc., Dalton Trans.* **1991**, 2253. (g) Usón, R.; Forniés, J.; Tomás, M.; Menjón, B.; Fortuño, C.; Welch, A. J.; Smith, D. E. *J. Chem. Soc., Dalton Trans.* **1993**, 275. (h) Casas, J. M.; Forniés, J.; Martín, A. *J. Chem. Soc., Dalton Trans.* **1997**, 1559. (i) Casas, J. M.; Forniés, J.; Martín, A.; Welch, A. J. *Inorg. Chem.* **1996**, *35*, 6009.

Scheme 1

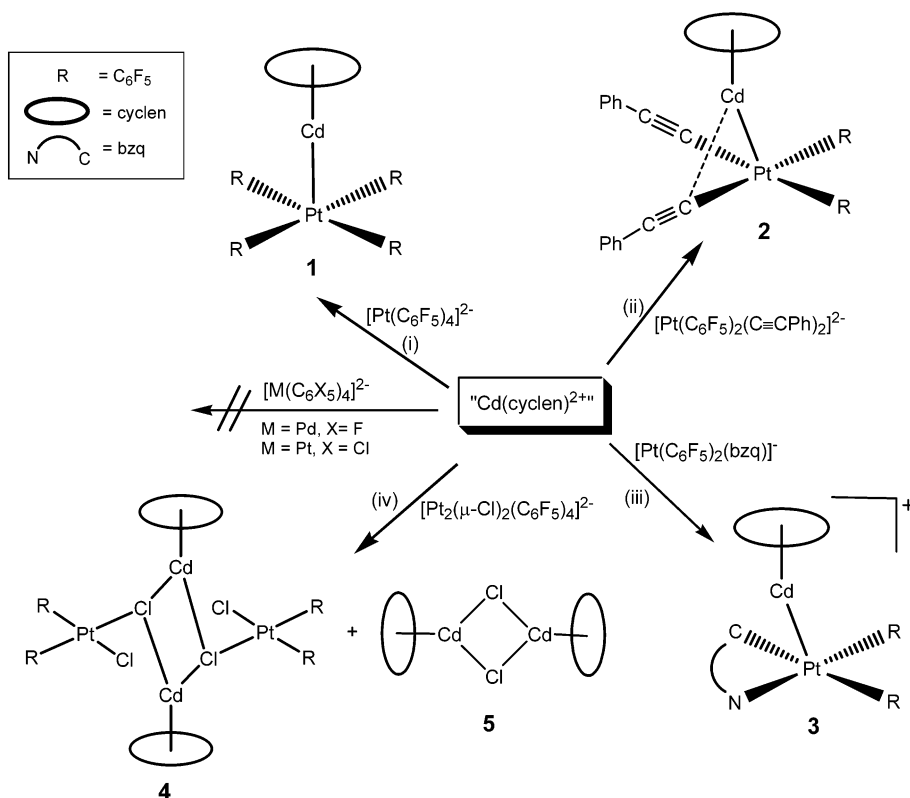


Table 1. Crystal Data and Structure Refinement for Complexes [(C₆F₅)₄PtCd(cyclen)]·2Me₂CO (1·2Me₂CO), [(C₆F₅)₂Pt(C≡CPh)₂Cd(cyclen)]·2Me₂CO (2·2Me₂CO), [(C₆F₅)₂(bzq)PtCd(cyclen)](ClO₄)·0.5MeOH (3·0.5MeOH), [Pt(C₆F₅)₂Cl₂Cd(cyclen)]₂·2Me₂CO (4·2Me₂CO), and [Cd₂(μ-Cl)₂(cyclen)₂](ClO₄)₂ (5)

	1·2Me ₂ CO	2·2Me ₂ CO	3·0.5MeOH	4·2Me ₂ CO	5
formula	C ₃₂ H ₂₀ CdF ₂₀ N ₄ Pt·2Me ₂ CO	C ₃₆ H ₃₀ CdF ₁₀ N ₄ Pt·2Me ₂ CO	C ₃₃ H ₂₄ CdClF ₁₀ N ₅ O ₄ ·Pt·0.5MeOH	C ₄₀ H ₄₀ Cd ₂ Cl ₄ F ₂₀ N ₈ Pt ₂ ·2Me ₂ CO	C ₁₆ H ₄₀ Cd ₂ Cl ₄ N ₈ O ₈
<i>a</i> [Å]	23.837(2)	16.5340(1)	12.7984(18)	9.7955(14)	12.5374(10)
<i>b</i> [Å]	9.9630(8)	19.2220(1)	17.239(3)	12.1984(18)	15.2365(13)
<i>c</i> [Å]	17.4955(15)	27.5390(2)	7.132(3)	12.6514(18)	15.5517(13)
α [deg]	90	90	90	79.633(3)	90
β [deg]	96.821(2)	90	90.239(3)	81.820(3)	90
γ [deg]	90	90	90	74.375(3)	90
<i>V</i> [Å ³], <i>Z</i>	4125.5(6), 4	8752.35(9), 8	3779.8(10), 4	1425.0(4), 1	2970.8(4), 4
ρ _{calc} [g cm ⁻³]	2.035	1.719	1.939	2.197	1.876
<i>T</i> [K]	173(1)	173(1)	293(1)	100(1)	173(1)
cryst syst	monoclinic	orthorhombic	monoclinic	triclinic	orthorhombic
space group	<i>C2/c</i>	<i>Pbca</i>	<i>P2₁/n</i>	<i>P1</i>	<i>Pnma</i>
dimensions [mm]	0.40 × 0.35 × 0.20	0.30 × 0.10 × 0.10	0.12 × 0.10 × 0.08	0.05 × 0.05 × 0.02	0.20 × 0.15 × 0.02
μ [mm ⁻¹]	4.034	3.761	4.425	5.929	1.844
abs corr	3219 symmetry equivalent reflns	semiempirical from equivalents	4477 symmetry equivalent reflns	3132 symmetry equivalent reflns	1696 symmetry equivalent reflns
θ range [deg]	1.72–24.87	2.12–27.89	1.68–25.10	1.64–25.04	2.09–24.87
no. of reflns collected	11 337	142 986	19 921	7828	6071
no. of indep reflns	3580 (<i>R</i> (int) = 0.0423)	10438 (<i>R</i> (int) = 0.0573)	6721 (<i>R</i> (int) = 0.0870)	4958 (<i>R</i> _{int} = 0.0302)	2685 (<i>R</i> _{int} = 0.0755)
final <i>R</i> indices [<i>I</i> > 2σ(<i>I</i>)] ^a	<i>R</i> 1 = 0.0340,	<i>R</i> 1 = 0.0371,	<i>R</i> 1 = 0.0516,	<i>R</i> 1 = 0.0440,	<i>R</i> 1 = 0.0433,
<i>R</i> indices (all data)	w <i>R</i> 2 = 0.0888 <i>R</i> 1 = 0.0391, w <i>R</i> 2 = 0.0982	w <i>R</i> 2 = 0.0912 <i>R</i> 1 = 0.0522, w <i>R</i> 2 = 0.0982	w <i>R</i> 2 = 0.1027 <i>R</i> 1 = 0.1384, w <i>R</i> 2 = 0.1163	w <i>R</i> 2 = 0.1114 <i>R</i> 1 = 0.0532, w <i>R</i> 2 = 0.1171	w <i>R</i> 2 = 0.0885 <i>R</i> 1 = 0.0655, w <i>R</i> 2 = 0.0945
goodness-of-fit on <i>F</i> ² ^b	1.029	1.075	1.037	1.001	0.903
largest diff peak/hole [e Å ⁻³]	1.17/–1.53	1.07/–0.93	1.03/–0.77	1.53/–1.46	0.80/–0.78

^a w*R*2 = [Σw(*F*_o² – *F*_c²)/Σw*F*_o⁴]^{0.5}; *R*1 = Σ||*F*_o| – |*F*_c||/Σ|*F*_o|. ^b Goodness-of-fit = [Σw(*F*_o² – *F*_c²)/(*N*_{obs} – *N*_{param})]^{0.5}.

longer than the distance found in [(phpy)₂PtCd(cyclen)](ClO₄)₂ (2.639(1) Å) and [(bpy)Me₂PtCd(cyclen)](ClO₄)₂ (2.610(1) Å) although shorter than the Pt···Cd interactions described in [NBu₄]₂{[Pt(μ-C≡CPh)₂(CdCl)₂]₂}³ and {[Pt₄Cd₆(C≡CPh)₄(μ-C≡CPh)₁₂(μ₃-OH)₄]}⁴. The Pt–

Cd bond is perpendicular to the best square planar environment of the Pt atom.

It is also important to mention that, although most of these pentafluorophenyl platinate (Pt→M) complexes display short *o*-F···M interactions (for instance in [NBu₄]-

Table 2. Selected Bond Lengths (Å) and Angles (deg) for [(C₆F₅)₄PtCd(cyclen)]·2Me₂CO (1·2Me₂CO)^a

Pt–C(7)	2.060(6)	Pt–C(1)	2.069(6)
Cd–N(1)	2.380(5)	Cd–N(2)	2.399(4)
Pt–Cd	2.775(1)		
C(7)–Pt–C(7')	172.2(3)	C(7)–Pt–C(1)	89.0(2)
C(7')–Pt–C(1)	90.5(2)	C(1)–Pt–C(1')	172.7(3)
C(7)–Pt–Cd	93.89(14)	C(1)–Pt–Cd	93.64(14)
N(1)–Cd–N(1')	117.7(2)	N(1)–Cd–N(2)	74.40(16)
N(1')–Cd–N(2)	74.98(16)	N(2)–Cd–N(2')	118.6(2)
N(1)–Cd–Pt	121.16(12)	N(2)–Cd–Pt	120.69(12)

^a The symmetry transformation used to generate equivalent primed atoms is 1–*x*, *y*, 1/2–*z*.

[(C₆F₅)₄PtAg(SC₄H₈)] (**A**)^{10f} the four *o*-F⋯Ag contacts range from 2.704(10) to 2.738(9) Å and could contribute to the stability of the Pt–M complex, in **1** all the *o*-F⋯Cd distances are longer than 3 Å, indicating that such contacts are not present. An additional indication of the lower interest of the Cd center to establish these contacts is that the pentafluorophenyl rings are forming dihedral angles with the platinum coordination plane of 52.2° (C(1)) and 55.3° (C(7)), while the corresponding angles in [NBu₄][(C₆F₅)₄PtAg(SC₄H₈)] (**A**) are 77.6°, 74.1°, 62.6°, and 62.0°, these latter values being obviously more adequate for forming *o*-F⋯M contacts.

Considering that in **1** the Pt–Cd distance is longer than the Pt–Ag one (2.641(1) Å in **A**; the metallic radii for Cd and Ag are similar, 1.49 and 1.45 Å, respectively) and than the Pt–Cd distances in [(phpy)₂PtCd(cyclen)](ClO₄)₂ and [(bpy)Me₂PtCd(cyclen)](ClO₄)₂, it is clear that the Pt–Cd bond in **1** is weaker than in other cases. This weakness could well be a consequence of the steric repulsion between the *o*-F atoms of the C₆F₅ rings and the donor atoms of the cyclen. Such repulsion should be much lower (if any) in the silver derivative [NBu₄][(C₆F₅)₄PtAg(SC₄H₈)] (**A**), while in Ito's complexes the planarity of the whole environment of the platinum center should favor the closing up of the acid and basic centers.

The IR spectrum of **1** shows bands corresponding to the cyclen and pentafluorophenyl ligands. The latter cause the presence of a sharp, strong band at 773 cm⁻¹, assignable to the X-sensitive mode of the C₆F₅ group, which is typical for a "Pt(C₆F₅)₄" moiety. The ¹H NMR (HDA) contains three signals due to the cyclen ligand. One is a broad band assignable to the four NH protons; the other two are complex multiplets, which integrate for 8 H each. The equivalence of the four pentafluorophenyl groups is observed in the ¹⁹F NMR spectrum (HDA). However, only three signals appear, both at room or low temperature, each one corresponding to the different types of fluorine atoms (*ortho*, *meta*, and *para*), typical of an AA'MM'X spin system.¹¹ The value of the conductivity of an acetone solution of complex **1** (42 Ω⁻¹ cm² mol⁻¹) indicates that it is a poor conductor in solution, and this could be indicating that the Pt–Cd bond exists even in a donor solvent such as acetone. In fact, suitable crystals for the X-ray structure determination of **1** were grown from acetone solutions.

The existence of a AA'MM'X spin system for the C₆F₅ groups in the ¹⁹F NMR spectrum of **1** seems to be due to a very fast dissociation equilibrium between **1** and the mononuclear starting material. If a small amount of [NBu₄]₂[Pt(C₆F₅)₄] is added to a HDA solution of **1** at

room temperature and the ¹⁹F NMR spectrum of this solution is recorded, no signals due to the mononuclear starting material are observed, and the only signal that appears in the *ortho* F region of the spectrum is displaced from that observed in the spectrum of pure **1**. This displacement occurs toward the chemical shift observed for the signal of pure [NBu₄]₂[Pt(C₆F₅)₄]. When a second fraction of [NBu₄]₂[Pt(C₆F₅)₄] is added to the solution mixture, the displacement of the *o*-F signal is even greater.

Attempts to prepare the analogous dinuclear complexes using [NBu₄]₂[Pd(C₆F₅)₄] or [NBu₄]₂[Pt(C₆Cl₅)₄] as donor precursors have not been successful. In the case of the palladium complex, only mixtures of the starting materials and unidentified decomposition products were recovered. In the case of the pentachlorophenyl derivative, no reaction took place and the unaltered platinum precursor was recovered. It seems reasonable to assume that the bulkier C₆Cl₅ ligands do not allow the Cd center close enough to the platinum center to establish the Pt–Cd bond.

A similar neutral platinum–cadmium complex [(C₆F₅)₂-(C≡CPh)₂PtCd(cyclen)] (**2**) is prepared using the dianionic bis(phenylethynyl)bis(pentafluorophenyl)platinate(II), [PMePh₃]₂[Pt(C₆F₅)₂(C≡CPh)₂]¹³ as starting material (Scheme iii). In this case, treatment of [PMePh₃]₂[Pt(C₆F₅)₂(C≡CPh)₂] with 1 equiv of cyclen and CdClO₄ in methanol produces the precipitation of the complex [(C₆F₅)₂(C≡CPh)₂PtCd(cyclen)] (**2**) as a very pale yellow microcrystalline solid in moderate yield (30%). Partial evaporation of the solvent from the filtrate gives a second fraction of complex (14%). The observation of two *ν*(C≡C) absorptions (2097, 2080 cm⁻¹) at a position similar to those observed in [PMePh₃]₂[Pt(C₆F₅)₂-(C≡CPh)₂] (2095, 2082 cm⁻¹)¹³ suggests that the interaction of the Cd center with the acetylenic fragments is probably weak. Additionally the IR and ¹H NMR spectra confirm the presence of cyclen and C≡CPh ligands. Conductivity measurements in acetone solution (3.3 Ω⁻¹ cm² mol⁻¹) indicate its behavior as a neutral compound.

Crystals suitable for a single-crystal X-ray diffraction study (Figure 2) were obtained by slow evaporation of an acetone solution of complex **2**. Under these conditions, the complex crystallizes as **2**·2Me₂CO. Selected crystallographic data and atomic distances and angles are listed in Tables 1 and 3, respectively. As can be observed in Figure 2, the compound is also formed by the expected units "Pt(C₆F₅)₂(C≡CPh)₂²⁻" and "Cd(cyclen)²⁺" connected through a Pt–Cd donor–acceptor bond. The Pt–Cd distance is only slightly shorter (2.764(1) Å) than the distance in **1** (2.775(1) Å). The most remarkable difference is the fact that in **2**, and probably due to the presence of the alkynyl entities, the Pt–Cd vector is perceptibly displaced from the normal to the platinum coordination plane (34.58(9)°) and located above the Pt–C(1)≡C(2) alkynyl fragment.

(11) For recent ¹⁹F NMR studies on pentafluorophenyl complexes see: Casares, J. A.; Espinet, P.; Martín-Alvarez, J. M.; Santos, V. *Inorg. Chem.* **2004**, *43*, 189. See also ref 12.

(12) (a) Alonso, M. A.; Casares, J. A.; Espinet, P.; Martínez-Illarduya, J. M.; Pérez-Briso, C. *Eur. J. Inorg. Chem.* **1998**, 1745, and references therein. (b) Casares, J. A.; Espinet, P.; Martínez de Illarduya, J. M.; Lin, Y.-S. *Organometallics* **1997**, *16*, 770.

(13) Espinet, P.; Forniés, J.; Martínez, F.; Sotés, M.; Lalinde, E.; Moreno, M. T.; Ruiz, A.; Welch, A. J. *J. Organomet. Chem.* **1991**, *403*, 253.

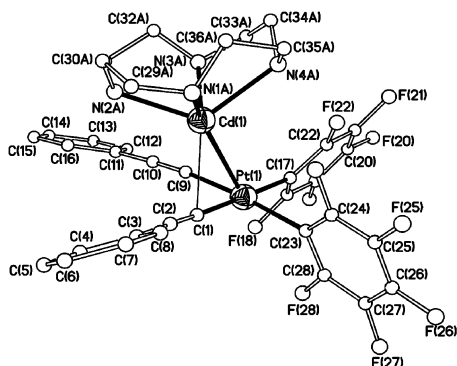


Figure 2. Structure of the complex $[(\text{C}_6\text{F}_5)_2\text{Pt}(\text{C}\equiv\text{CPh})_2\text{Cd}(\text{cyclen})]$ (**2**). For the sake of clarity, only the cyclen atoms of one of the components of the disorder (see Experimental Section) are shown.

Table 3. Selected Bond Lengths (Å) and Angles (deg) for $[(\text{C}_6\text{F}_5)_2\text{Pt}(\text{C}\equiv\text{CPh})_2\text{Cd}(\text{cyclen})]\cdot 2\text{Me}_2\text{CO}$ ($2\cdot 2\text{Me}_2\text{CO}$)

Pt–C(1)	2.011(5)	Pt–C(9)	2.015(5)
Pt–C(17)	2.062(5)	Pt–Cd	2.764(1)
Cd–N(1a)	2.332(9)	Cd–N(3a)	2.359(5)
Pt–C(23)	2.065(5)	Cd–N(4a)	2.420(7)
Cd–N(2a)	2.289(6)		
C(1)–Pt–C(9)	92.50(18)	C(1)–Pt–Cd	60.53(12)
C(1)–Pt–C(23)	88.23(19)	C(9)–Pt–Cd	75.17(12)
C(9)–Pt–C(17)	89.69(19)	C(23)–Pt–Cd	109.94(14)
C(23)–Pt–C(17)	89.9(2)	C(17)–Pt–Cd	117.52(15)
C(2)–C(1)–Pt	174.1(4)	C(10)–C(9)–Pt	173.9(4)
C(1)–C(2)–C(3)	178.4(5)	C(9)–C(10)–C(11)	177.5(5)

As a consequence, the Cd center is in a more complicated environment formed by the four nitrogen atoms of the cyclen ligand, the Pt atom, and the C_α carbon of one of the two alkynyl groups. The very acute Cd–Pt–C(1) bond angle ($60.53(12)^\circ$) and, particularly, the Cd–C(1) carbon length (2.493 Å), which is comparable to those observed in the anions $[\{\text{Pt}(\mu\text{-}\eta^1\text{-C}\equiv\text{CPh})_4\}_2(\text{CdCl})_2]^{2-}$ and $[\{\text{Pt}(\mu\text{-}\eta^2\text{-C}\equiv\text{CPh})_4\}(\text{CdCl}_2)_2]^{2-}$ (2.403(11)–2.657(12) Å),³ indicate that the C(1)≡C(2)–Ph fragment is acting as a $\mu\text{-}\eta^1$ alkynyl bridging ligand. The structural details for the alkynyl fragments are unexceptional for this type of ligand.² The remaining Cd–acetylenic carbon (Cd–C(2) 2.98 Å, Cd–C(9) 2.97 Å) and the shortest Cd–fluorine-ortho (Cd–F(24) 3.299 Å) distances are very long, excluding other bonding interactions. The dihedral angle of the C_6F_5 ring containing the F(24) atom with the platinum coordination plane is slightly larger ($71.14(18)^\circ$) than the angle formed for the C_6F_5 ring *trans* to the $\mu\text{-}\eta^1\text{-C}\equiv\text{CPh}$ ligand ($65.04(20)^\circ$), and both are clearly more perpendicular to the Pt plane than those seen in **1**. It seems also clear that the location of the “Cd(cyclen)²⁺” moiety toward the acetylide ligands prevents the repulsion of the *ortho*-fluorine atoms of the C_6F_5 group and the “Cd(cyclen)²⁺” moiety. A view along the *a* axis of the crystal lattice reveals the existence of square channels formed for the pentafluorophenyl rings in which the acetone molecules are placed (see Figure 1S in the Supporting Information). Although no contact between these solvent molecules and any of the fluorine atoms is observed, their presence plays an important role in the luminescence of this complex (see below).

Fluxional behavior of complex **2** in solution is evident by ^{19}F NMR spectroscopy. At room temperature, it

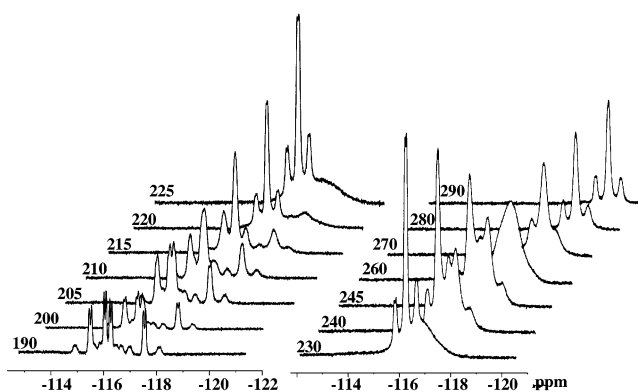


Figure 3. Variable-temperature ^{19}F NMR spectra (*ortho*-fluorine region) of $[(\text{C}_6\text{F}_5)_2\text{Pt}(\text{C}\equiv\text{CPh})_2\text{Cd}(\text{cyclen})]$ (**2**).

displays only one set of C_6F_5 -fluorine signals [*o*-F: 3(1-*p*-F, 2-*m*-F)], thus confirming that both C_6F_5 rings are equivalent and indicating the effective equivalence of the *o*-F atom and the *m*-F as well. However, as can be seen in Figure 3, which shows the *ortho*-fluorine region at different temperatures, in acetone-*d*₆, the pattern observed at 190 K is that expected for a rigid molecule. The presence of four *ortho*-fluorine resonances indicates the existence of two different C_6F_5 rings with their halves nonequivalent, thus confirming that the possible exchange of the “Pt(cyclen)” unit between both alkynyl ligands is slow on the NMR time scale and that the rotation of the C_6F_5 groups around the Pt–C_{ipso} bond is also hindered. Increasing the monitoring temperatures resulted in a clear broadening of the *o*-fluorine resonances. The two central signals [–116.0, d, $J_{\text{F-F}} = 30$ Hz; –116.3, d, $J_{\text{F-F}} = 26$ Hz] coalesce at about 208 K and finally collapse to only one, centered at –116.2 at 220 K, while the external ones [–115.5, d, $J_{\text{F-F}} = 30$ Hz; –117.5, d, $J_{\text{F-F}} = 26$ Hz] coalesce at about 228 K and average to one, centered at –116.7 at 240 K. The ΔG^\ddagger for both pairs of signals at their coalescence temperature are similar (central $\Delta G^\ddagger \approx 41.20$ kJ/mol; external $\Delta G^\ddagger \approx 41.1$ kJ/mol), suggesting that they are involved in the same dynamic process. The external resonances, which are seen as doublets with *ortho*–*meta*-fluorine coupling constants of 30 and 26 Hz, are tentatively assigned to *endo* *ortho*-fluorine atoms of different C_6F_5 rings, and therefore the central signals are attributed to the corresponding two *exo*-fluorine atoms. The observed equilibration of both C_6F_5 groups (average of *endo* with *endo* and *exo* with *exo* fluorine atoms of each ring) at 240 K can be explained by assuming a fast exchange of the Cd(cyclen) fragment between both alkynyl ligands on the NMR time scale. Above 245 K, the two *ortho*-fluorine resonances broaden again, coalesce near 260 K, and finally collapse to only one, centered at –117.2 at 270 K, requiring the consideration of an additional dynamic process. As for complex **1**, free rotation of the rings along the Pt–C_{ipso}(C_6F_5) bond or a fast and facile dissociation of the Cd(cyclen) unit or a combination of both processes could adequately explain such changes. However in this case, at 240 K, the addition of a small amount of $[\text{PMePh}_3]_2[\text{Pt}(\text{C}_6\text{F}_5)_2(\text{C}\equiv\text{CPh})_2]$ gives rise to a ^{19}F NMR spectrum containing separate signals of **2** and the starting material, thus indicating that in **2** dissociation of the Cd(cyclen) unit does not occur or it is very slow on the NMR time scale.

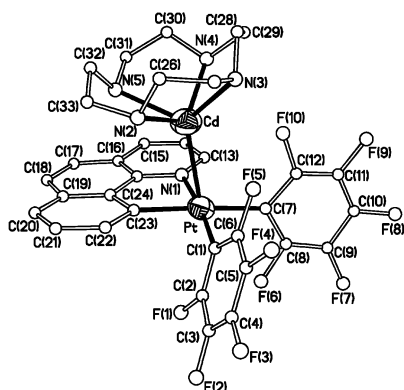


Figure 4. Structure of the cation of the complex $[(\text{C}_6\text{F}_5)_2\text{-}(\text{bzq})\text{PtCd}(\text{cyclen})](\text{ClO}_4)$ (**3**).

However, on raising the temperature (to 300 K), the signals due to $[\text{PMePh}_3]_2[\text{Pt}(\text{C}_6\text{F}_5)_2(\text{C}\equiv\text{CPh})_2]$ disappear on the baseline and the only signal observed in the *ortho*-fluorine region appears broader, suggesting a possible fast equilibrium between **2** and $[\text{PMePh}_3]_2\text{-}[\text{Pt}(\text{C}_6\text{F}_5)_2(\text{C}\equiv\text{CPh})_2]$ at high temperature.

Synthesis of $[(\text{C}_6\text{F}_5)_2(\text{bzq})\text{PtCd}(\text{cyclen})](\text{ClO}_4)$ (3**).** We have also studied the reaction of the cationic fragment “ $\text{Cd}(\text{cyclen})^{2+}$ ” toward the monoanionic complex $[\text{Pt}(\text{C}_6\text{F}_5)_2(\text{bzq})]^-$ (bzq = 7,8-benzoquinolate, see Chart 1), which contains two pentafluorophenyl rings mutually *cis* and a bidentate anionic ligand *bzq* (Scheme 1iii). The latter ligand is planar, and thus, in principle, there is less steric hindrance for the cadmium atom to approach the Pt center to establish an intermetallic bond. The required precursor $[\text{NBu}_4][\text{Pt}(\text{C}_6\text{F}_5)_2(\text{bzq})]$ (**6**) was prepared from $[\text{NBu}_4][\text{Pt}(\text{C}_6\text{F}_5)_3(7,8\text{-benzoquinoline})]$ by thermal-induced deprotonation of the *bzqH* ligand in CH_2Cl_2 at reflux temperature (3 h) (see Experimental Section for details) and fully characterized by elemental analysis and IR and NMR (^1H , ^{19}F) spectroscopy. The NMR data unambiguously reveal the presence of the *bzq* ligand and the unequivalence of both C_6F_5 rings.

Treatment of **6** with a MeOH solution of $[\text{Cd}(\text{cyclen})\text{-}(\text{MeOH})_2](\text{ClO}_4)_2$, prepared in situ, in 1:1 molar ratio, gives the binuclear cationic complex $[(\text{C}_6\text{F}_5)_2(\text{bzq})\text{PtCd}(\text{cyclen})](\text{ClO}_4)$ (**3**) as a yellow solid. Its IR spectrum shows, in the X-sensitive region, in addition to the two expected typical sharp absorptions due to the presence of the two mutually *cis* pentafluorophenyl rings, signals due to *bzq* and *cyclen* ligands. In the ^{19}F NMR spectrum, the inequivalence of the two pentafluorophenyl groups is confirmed, each C_6F_5 forming a $\text{AA}'\text{MM}'\text{X}$ spin system. Conductivity measurements in acetone solutions of complex **3** confirm its behavior as a 1:1 electrolyte (see Experimental Section). This would indicate that the Pt–Cd bond persists even in a donor solvent such as acetone. ^{19}F NMR studies similar to the ones described for **1** have been carried out with similar results, indicating that a dissociative equilibrium is taking place in solution.

The crystal structure of the cation of **3** is shown in Figure 4. Crystallographic data are given in Table 1, and selected interatomic distances and angles appear in Table 4. The dinuclear cation **3** can be described as the union of the moieties “ $\text{Pt}(\text{C}_6\text{F}_5)_2(\text{bzq})$ ” and “ $\text{Cd}(\text{cyclen})$ ” through a Pt–Cd donor–acceptor bond. The

Table 4. Selected Bond Lengths (Å) and Angles (deg) for $[(\text{C}_6\text{F}_5)_2(\text{bzq})\text{PtCd}(\text{cyclen})](\text{ClO}_4)\cdot 0.5\text{MeOH}$ (**3**·0.5MeOH)

Pt–C(7)	1.985(14)	Pt–C(23)	1.986(12)
Pt–N(1)	2.065(10)	Pt–Cd	2.688(1)
Cd–N(3)	2.337(10)	Cd–N(2)	2.348(12)
Pt–C(1)	2.011(11)	Cd–N(5)	2.361(13)
Cd–N(4)	2.334(13)		
C(7)–Pt–C(23)	173.6(5)	C(7)–Pt–C(1)	90.2(5)
C(23)–Pt–C(1)	93.3(5)	C(7)–Pt–N(1)	94.8(5)
C(23)–Pt–N(1)	81.3(5)	C(1)–Pt–N(1)	173.3(5)
C(7)–Pt–Cd	104.5(5)	C(23)–Pt–Cd	79.7(3)
C(1)–Pt–Cd	105.7(4)	N(1)–Pt–Cd	77.5(3)
N(4)–Cd–N(3)	78.2(5)	N(4)–Cd–N(2)	123.9(5)
N(3)–Cd–N(2)	76.4(5)	N(4)–Cd–N(5)	75.8(5)
N(3)–Cd–N(5)	119.7(5)	N(2)–Cd–N(5)	75.0(6)
N(4)–Cd–Pt	123.8(3)	N(3)–Cd–Pt	124.1(3)
N(2)–Cd–Pt	111.9(3)	N(5)–Cd–Pt	115.6(4)

Pt–Cd distance is 2.688(1) Å, slightly shorter than those observed in **1** and **2**, but still longer than those found in $[(\text{phpy})_2\text{PtCd}(\text{cyclen})](\text{ClO}_4)_2$ (2.639(1) Å) and $[(\text{bpy})\text{Me}_2\text{-PtCd}(\text{cyclen})](\text{ClO}_4)_2$ (2.610(1) Å).⁵ The geometry of the “ $\text{Cd}(\text{cyclen})$ ” fragment is as in complexes **1** and **2**. The Pt atom and the four atoms coordinated to it in its square planar environment lie basically on the same plane. The 7,8-benzoquinolate ligand is also essentially planar, forming a dihedral angle of 10.2(3)° with the Pt square plane in such a way that it moves away from the Cd. The angle formed by the Pt–Cd line with the perpendicular to the best Pt coordination square plane takes an intermediate value (17.6(2)°) to that of the same angles in the neutral complexes **1** (0°) and **2** (34.58(9)°). This line leans away from the perpendicular toward the planar 7,8-benzoquinolate ligand in such a way that the Cd atom moves away from the pentafluorophenyl groups. As a concomitant result, the C_6F_5 planes form angles with the Pt coordination square plane of 70.6(4)° (C(1)) and 78.6(4)° (C(7)) (cf. 52.2° (C(1)) and 55.3° (C(7)) in **1**); that is, they are more perpendicular to the Pt plane than for complex **1**. The shortest Cd–F distance is 2.966(9) Å, established with F(10); although this separation is shorter than the sum of van der Waals radii (3.10–3.20 Å),¹⁴ it is still too long to be considered as an *o*-F⋯Cd contact.

Comparison of the crystal structures of **1**, **2**, and **3** seems to indicate that there is a steric repulsion between the pentafluorophenyl groups attached to the platinum and the bulky *cyclen* ligand coordinated to the cadmium. For **1**, the presence of four C_6F_5 ligands around the platinum causes the Pt–Cd distance to be longer, while in **2** and **3** the Cd fragment can approach the Pt center better due to the presence of linear alkynyl fragments or the planar 7,8-benzoquinolate ligand moving away from the C_6F_5 groups. It is also interesting to mention that in **2** the interaction between “ $\text{Cd}(\text{cyclen})$ ” and one acetylide ligand could also favor the angle between the perpendicular to the Pt coordination plane and the Pt–Cd bond being greater than in **3**.

Reaction of $[\text{NBu}_4]_2[\text{Pt}_2(\mu\text{-Cl})_2(\text{C}_6\text{F}_5)_4]$ with $[\text{Cd}(\text{cyclen})(\text{MeOH})_2](\text{ClO}_4)_2$. With the aim of preparing a trinuclear complex¹⁵ in which the binuclear $[\text{Pt}_2(\mu\text{-Cl})_2(\text{C}_6\text{F}_5)_4]^{2-}$ moiety could act as a bidentate chelating ligand and two Pt–Cd bonds would be present, we performed the reaction of $[\text{NBu}_4]_2[\text{Pt}_2(\mu\text{-Cl})_2(\text{C}_6\text{F}_5)_4]$ with

(14) Bondi, A. *J. Phys. Chem.* **1964**, *68*, 441.

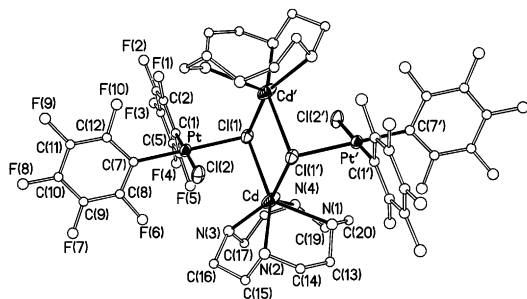


Figure 5. Structure of the complex $[\text{Pt}(\text{C}_6\text{F}_5)_2\text{Cl}_2\text{Cd}(\text{cyclen})]_2$ (**4**). For the sake of clarity, only the cyclen atoms of the major component of the disorder (see Experimental Section) are shown.

Table 5. Selected Bond Lengths (Å) and Angles (deg) for $[\text{Pt}(\text{C}_6\text{F}_5)_2\text{Cl}_2\text{Cd}(\text{cyclen})]_2 \cdot 2\text{Me}_2\text{CO}$ (4**·2Me₂CO)^a**

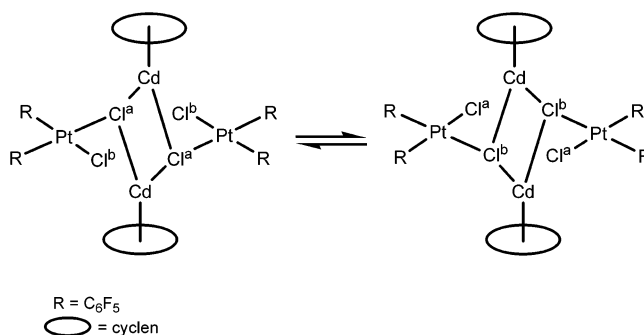
Pt–C(7)	1.982(8)	Pt–C(1)	1.991(8)
Pt–Cl(1)	2.400(2)	Cd–N(2)	2.319(9)
Cd–N(1)	2.417(9)	Cd–N(4)	2.420(9)
Cd–Cl(1)	2.840(2)	Cd–Cl(1')	2.655(2)
Pt–Cl(2)	2.386(2)	Cd–N(3)	2.323(9)
C(7)–Pt–C(1)	87.3(3)	C(7)–Pt–Cl(2)	92.6(2)
C(1)–Pt–Cl(2)	178.5(2)	C(7)–Pt–Cl(1)	178.7(2)
C(1)–Pt–Cl(1)	91.5(2)	Cl(2)–Pt–Cl(1)	88.61(7)
N(2)–Cd–N(3)	79.3(4)	N(2)–Cd–N(1)	75.4(4)
N(3)–Cd–N(1)	118.6(4)	N(2)–Cd–N(4)	119.2(4)
N(3)–Cd–N(4)	74.4(4)	N(1)–Cd–N(4)	71.2(3)
N(2)–Cd–Cl(1')	94.8(3)	N(3)–Cd–Cl(1')	153.1(3)
N(1)–Cd–Cl(1')	84.5(3)	N(4)–Cd–Cl(1')	129.6(3)
N(2)–Cd–Cl(1)	155.2(2)	N(3)–Cd–Cl(1)	89.1(3)
N(1)–Cd–Cl(1)	129.1(3)	N(4)–Cd–Cl(1)	77.6(3)
Cl(1')–Cd–Cl(1)	85.57(6)	Pt–Cl(1)–Cd'	106.93(7)
Pt–Cl(1)–Cd	92.73(7)	Cd'–Cl(1)–Cd	94.43(6)

^a The symmetry transformation used to generate equivalent primed atoms is $-x, -y, -z$. For the sake of clarity, only the cyclen atoms of the major component of the disorder (see Experimental Section) are included.

$[\text{Cd}(\text{cyclen})(\text{MeOH})_2](\text{ClO}_4)_2$ in 1:1 molar ratio (Scheme 1iv). When the dinuclear platinum complex was added to a MeOH solution of $[\text{Cd}(\text{cyclen})(\text{MeOH})_2](\text{ClO}_4)_2$, a white suspension appeared due to the insolubility of the Pt complex in methanol. This suspension was stirred for 1 h, and then the white solid was filtered off and vacuum-dried. The stoichiometry of this material was not clear. The elemental analysis did not coincide with that calculated for the expected $[(\text{C}_6\text{F}_5)_4(\mu\text{-Cl})_2\text{Pt}_2\text{Cd}(\text{cyclen})]$ formula (see Experimental Section).

A single-crystal X-ray study allowed us to determine the solid-state structure of this complex, $[\text{Pt}(\text{C}_6\text{F}_5)_2\text{Cl}_2\text{Cd}(\text{cyclen})]_2$ (**4**). The structure is shown in Figure 5. Crystallographic data are given in Table 1, and selected interatomic distances and angles appear in Table 5. **4** is a tetranuclear compound without Pt–Cd bonds and with two chlorine atoms acting as a μ_3 ligand, bridging two Cd and one Pt center. The platinum atoms lie in the center of square planar environments formed by two pentafluorophenyl ligands and two chlorine atoms in a *cis* disposition. One of the chlorine atoms acts as a terminal ligand, while the other is bridging the platinum atom with the two cadmium atoms present in the complex. The Cd atoms are six coordinated and have a cyclen ligand coordinated in the usual way. The long Pt–Cd distances (3.805(1) Å for Cd and 4.065(1) Å for Cd') exclude any kind of intermetallic interaction. Whereas the two Pt–Cl distances are very similar

Scheme 2



(Pt–Cl(2) = 2.386(2) Å, Pt–Cl(1) = 2.400(2) Å), the two Cd–Cl distances are perceptibly different: Cd–Cl(1) = 2.840(2) Å, Cd–Cl(1') = 2.655(2) Å. The first one is somewhat long, but there are some reported examples of similar long Cd–Cl distances in complexes in which the Cl atoms are bridging three metal atoms.¹⁶ It is noteworthy that the bridging Pt–Cl(1) distance is slightly shorter than the terminal Pt–Cl(2) length. Finally, the Pt square coordination planes are not perpendicular to the “Cd₂Cl₂” cycle (which is perfectly planar) but forms a dihedral angle of 101.9(1)°.

The solid-state structure found in the crystal cannot account for the ¹⁹F NMR spectrum of **4**, in which only signals due to one type of C₆F₅ group are observed. Should the structure in solution be the same as that in the solid state, two types of pentafluorophenyl groups should be observed in the ¹⁹F NMR spectrum. One possible explanation that could combine both experimental observations would be the existence of dynamic processes in solution, faster than the NMR time scale, and which would involve the rupture and formation of Cd–Cl bonds (see Scheme 2).

The different behavior of the acidic $[\text{Cd}(\text{cyclen})]^{2+}$ moiety toward $[\text{NBu}_4]_2[\text{Pt}(\text{C}_6\text{F}_5)_4]$ or $[\text{NBu}_4]_2[\text{Pt}_2(\mu\text{-Cl})_2(\text{C}_6\text{F}_5)_4]$ is noteworthy. Thus, when the main basic center present in the platinum complex is the metal itself, the reaction leads to the formation of **1**, a complex with a donor–acceptor Pt–Cd bond. On the other hand, when there are other basic centers, such as the chlorine atoms, they compete with each other with the result, in this case, that the formation of Cd–Cl bonds is preferred. Moreover, the reaction of formation of **4** implies the existence of processes of asymmetric breaking of the bridging system in the dinuclear starting material $[\text{NBu}_4]_2[\text{Pt}_2(\mu\text{-Cl})_2(\text{C}_6\text{F}_5)_4]$. The relatively low yield in the preparation of **4** (29%) indicates that there have to be other products formed in this reaction. So far, we have been able to identify and characterize only one of these products, $[\text{Cd}_2(\mu\text{-Cl})_2(\text{cyclen})_2](\text{ClO}_4)_2$ (**5**), of which suitable crystals for an X-ray structure determination were obtained during one of the attempts to crystallize **4**. Later, we were able to design a convenient synthetic procedure to prepare **5** starting from $[\text{Cd}(\text{cyclen})(\text{MeOH})_2](\text{ClO}_4)_2$ and $(\text{NBu}_4)\text{Cl}$ (see Experimental Section). The structure of the cation of **5** is shown

(15) Usón, R.; Forniés, J.; Tomás, M.; Casas, J. M.; Cotton, F. A.; Falvello, L. R. *Inorg. Chem.* **1987**, *26*, 3482.

(16) (a) Kubiak, M.; Glowiak, T.; Kozłowski, H. *Acta Crystallogr., Sect. C* **1989**, *39*, 1637. (b) Fawcett, T. G.; Ou, C. C.; Potenza, J. A.; Schugar, H. J. *J. Am. Chem. Soc.* **1978**, *100*, 2058. (c) Corradi, A. B.; Cramarossa, M. R.; Pellacani, G. C.; Battaglia, L. P.; Giusti, J. *Gazz. Chem. Ital.* **1994**, *124*, 481.

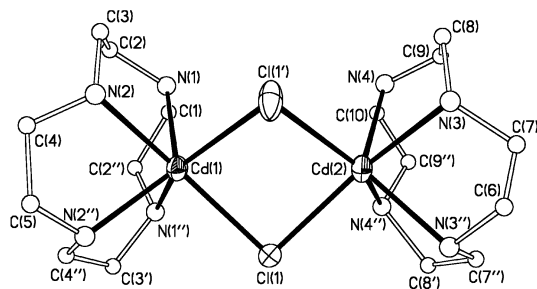


Figure 6. Structure of the cation of complex $[\text{Cd}_2(\mu\text{-Cl})_2(\text{cyclen})_2](\text{ClO}_4)_2$ (**5**). For the sake of clarity, only the cyclen atoms of one of the components of the disorder (see Experimental Section) are shown.

Table 6. Selected Bond Lengths (Å) and Angles (deg) for $[\text{Cd}_2(\mu\text{-Cl})_2(\text{cyclen})_2](\text{ClO}_4)_2$ (5**)^a**

Cd(1)–N(2)	2.365(11)	Cd(1)–N(1)	2.394(12)
Cd(2)–N(4)	2.388(14)	Cd(2)–N(3)	2.418(15)
Cd(1)–Cl(1)	2.6177(19)	Cd(2)–Cl(1)	2.6012(19)
N(2)–Cd(1)–N(1)	75.2(3)	N(2)–Cd(1)–Cl(1')	87.6(3)
N(1)–Cd(1)–Cl(1')	91.3(3)	N(2)–Cd(1)–Cl(1)	155.2(3)
N(2)–Cd(1)–Cl(1)	87.6(3)	N(1)–Cd(1)–Cl(1)	126.6(3)
N(1)–Cd(1)–Cl(1)	91.3(3)	Cl(1')–Cd(1)–Cl(1)	80.82(9)
N(4)–Cd(2)–N(3)	73.9(4)	N(4)–Cd(2)–Cl(1')	93.6(3)
N(3)–Cd(2)–Cl(1')	88.2(3)	N(4)–Cd(2)–Cl(1)	131.1(3)
N(4)–Cd(2)–Cl(1)	93.6(3)	N(3)–Cd(2)–Cl(1)	153.3(3)
Cl(1')–Cd(2)–Cl(1)	81.44(9)	Cd(2)–Cl(1)–Cd(1)	93.04(6)

^a For the sake of clarity, only the cyclen atoms of one of the components of the disorder (see Experimental Section) are included.

in Figure 6. Crystallographic data are given in Table 1, and selected interatomic distances and angles appear in Table 6. **5** is a dinuclear complex in which the two “Cd(cyclen)” fragments are bridged by two chlorine atoms. The most remarkable feature of this structure is the high value of the dihedral angle formed by the two planes defined by one Cd atom and the two bridging Cl. This angle takes a value of $34.4(1)^\circ$ and is the broadest of those reported for “Cd($\mu\text{-Cl}$)₂Cd” systems with no other bridging ligand linking the metal atoms.¹⁷

Absorption and Emission Spectroscopic Results for Complexes 1–3. Whereas photochemistry and photophysics of discrete $d^8\dots d^8$, $d^{10}\dots d^{10}$ binuclear systems have been extensively studied,^{7,8a,b,d,h,i} relatively little attention has been paid to mixed metal $d^8\dots d^{10}$ compounds. Most of these studies have been reported for systems containing closed-shell d^{10} monovalent coinage (Cu, Ag, Au) ions,^{2b,d,e,8j,18} and surprisingly very few spectroscopic investigations have been carried out for related d^{10} divalent metal ions. We have previously suggested that Pt \cdots Cd(II) interactions play an important role in interpreting the luminescence properties of tetranuclear dianionic $[\{\text{Pt}(\mu\text{-}C^{\alpha}\text{-}C^{\beta}\text{-}C\equiv\text{CPh})_4\}_2(\text{CdX})_2]^{2-}$ clusters.^{3,4} To gain further insights into the involvement of metal \cdots metal bonding interactions in the excited-state properties of these complexes, the optical properties of **1–3** and those of their precursors have been investigated (Tables 7 and 8).

The absorption spectrum of **1** shows, in CH_2Cl_2 , a low-energy absorption at 345 nm, which is related to the

Table 7. Absorption for Complexes ($\sim 5 \times 10^{-5}$ M solutions)

compound	absorption/nm ($10^3 \epsilon/\text{M}^{-1} \text{cm}^{-1}$)
$[\text{NBu}_4]_2[\text{Pt}(\text{C}_6\text{F}_5)_4]$	215(15.0), 326(3.2) acetone 236(48.77), 290sh(12.7) CH_2Cl_2
$[(\text{C}_6\text{F}_5)_4\text{PtCd}(\text{cyclen})]$ (1)	211(10.5), 327(7.2), 390sh(2.2) acetone 239(14.7), 297(8.8), 345(6.8) CH_2Cl_2
$[\text{PMePh}_3]_2[\text{Pt}(\text{C}_6\text{F}_5)_2\text{-}(\text{C}\equiv\text{CPh})_2]$	329(11.8) acetone 232(42.8), 275(22.6), 290(21.8), 310(19.2), 325(12.4) CH_2Cl_2
$[(\text{C}_6\text{F}_5)_2(\text{C}\equiv\text{CPh})_2\text{PtCd}(\text{cyclen})]$ (2)	327(1.5) acetone 230(25.6), 267(28.6), 280sh(25.3), 325(26.2), 349sh(10.7) CH_2Cl_2
$[\text{NBu}_4][\text{Pt}(\text{C}_6\text{F}_5)_2(\text{bzq})]$ (6)	215(21), 328(13.4), 344(12.0), 393(8.4), 422sh(5.8) acetone 243(66.4), 260(58.4), 315(27.5), 345(20.1), 380(12.1), 425(6.9) CH_2Cl_2
$[(\text{C}_6\text{F}_5)_2(\text{bzq})\text{PtCd}(\text{cyclen})\text{-}[\text{ClO}_4]$ (3)	220(27.0), 328(12.8), 393(6.8) acetone 225(9.5), 242(14.3), 280(8.2), 325(5.2), 375(3.3), 410(2.7) CH_2Cl_2

presence of the cadmium atom, apart from those at 239 and 297 nm related to those observed for $[\text{NBu}_4]_2[\text{Pt}(\text{C}_6\text{F}_5)_4]$ at 236 and 290 nm. These high-energy bands with a coefficient of extinction on the order of $10^4 \text{ M}^{-1} \text{ cm}^{-1}$ are as expected for predominantly ligand-centered (C_6F_5) transitions (^1LC).¹⁹ The absorption spectrum of the precursor compound $[\text{NBu}_4][\text{Pt}(\text{C}_6\text{F}_5)_2(\text{bzq})]$ (**6**) in CH_2Cl_2 contains high-energy bands (243–380 nm) due to ligand-centered transitions (^1LC , $\pi\text{-}\pi^*$ bzq, C_6F_5) with metal perturbation and a low-energy band at 425 nm ($\lambda = 422$ nm in acetone) which, in accordance with similar assignments,²⁰ can be tentatively attributed to a spin-allowed metal to ligand ($^1\text{MLCT Pt(d)}\text{-}\pi^*\text{bzq}^*$) transition. For the binuclear cationic complex $[(\text{C}_6\text{F}_5)_2(\text{bzq})\text{PtCd}(\text{cyclen})](\text{ClO}_4)$ (**3**), the low-energy band observed in **6** at 425 nm in CH_2Cl_2 is blue-shifted to 410 nm and in acetone is overlapped with the high-energy bands. This fact is consistent with the formation of the Pt–Cd donor \rightarrow acceptor bond, which produces an increase in the electrophilicity of the Pt metal center, resulting in a blue-shift for the MLCT absorption. Comparison of the absorption spectrum of complex **2** with the spectrum of $[\text{PMePh}_3]_2[\text{Pt}(\text{C}_6\text{F}_5)_2(\text{C}\equiv\text{CPh})_2]$ is less illustrative in relation to the Pt–Cd bonding interaction. In acetone solution, the band observed with a peak maximum at 329 nm ($\epsilon = 11\,790 \text{ M}^{-1} \text{ cm}^{-1}$) is only slightly blue-shifted in the binuclear complex $[(\text{C}_6\text{F}_5)_2(\text{C}\equiv\text{CPh})_2\text{PtCd}(\text{cyclen})]$ (**2**) (327 nm), although the extinction coefficient is smaller ($1520 \text{ M}^{-1} \text{ cm}^{-1}$). In

(18) (a) Balch, A. L.; Catalano, V. J.; Olmstead, M. M. *Inorg. Chem.* **1990**, *29*, 585. (b) Balch, A. L.; Catalano, V. J. *Inorg. Chem.* **1991**, *30*, 1302. (c) Yip, H. K.; Che, C. M.; Peng, S. M. *J. Chem. Soc., Chem. Commun.* **1991**, 1626. (d) Yip, H. K.; Lin, H. M.; Cheung, K. K.; Che, C. M.; Wang, Y. *Inorg. Chem.* **1994**, *33*, 1644. (e) Yip, H. K.; Lin, H. M.; Wang, Y.; Che, C. M. *J. Chem. Soc., Dalton Trans.* **1993**, 2939. (f) Yip, H. K.; Lin, H. M.; Wang, Y.; Che, C. M. *Inorg. Chem.* **1993**, *32*, 3402. (g) Pettijohn, C. N.; Jochowitz, E. B.; Chuong, B.; Nagle, J. K.; Vogler, A. *Coord. Chem. Rev.* **1998**, *171*, 85. (h) Xia, B. H.; Zhang, H. X.; Che, C. M.; Leung, K. H.; Phillips, D. L.; Zhu, N.; Zhou, Z. Y. *J. Am. Chem. Soc.* **2003**, *125*, 10362, and references therein.

(19) The absorption spectrum of BrC_6F_5 shows similar energy bands at 227 (11.3), 245 (15.6), 263 (16.6), and 285 (54.80) nm. The cyclen ligand also shows high-energy bands at 229 (6.78), 263 (2.98), and 269 (3.10) nm ($\epsilon \times 10^3 \text{ M}^{-1} \text{ cm}^{-1}$).

(20) (a) Balashev, K. P.; Puzyk, M. V.; Kotlyar, V. S.; Kulikova, M. V. *Coord. Chem. Rev.* **1997**, *15*, 109. (b) Lai, S. W.; Lam, H. W.; Cheung, K. K.; Che, C. M. *Organometallics* **2002**, *21*, 226. (c) Williams, J. A. G.; Beeby, A.; Davie, E. S.; Weinstein, J. A.; Wilson, C. *Inorg. Chem.* **2003**, *42*, 8609. (d) Jude, H.; Krause, J. A.; Connick, W. B. *Inorg. Chem.* **2004**, *43*, 725.

(17) See for example: (a) Zompa, L. J.; Díaz, H.; Margulis, T. N. *Inorg. Chim. Acta* **1995**, *232*, 131. (b) Braunstein, P.; Douce, L.; Knorr, M.; Strampfer, M.; Lanfranchi, M.; Tiripicchio, A. *J. Chem. Soc., Dalton Trans.* **1992**, 331. (c) Corradi, A. B.; Cramarossa, M. R.; Saladini, M. *Inorg. Chim. Acta* **1997**, *257*, 19. (d) Allred, R. A.; MacAlexander, L. H.; Arif, A. M.; Berreau, L. M. *Inorg. Chem.* **2002**, *41*, 6790.

Table 8. Photophysical Data for Complexes in Solid, KBr, and 10⁻³ M Solutions

compound	(T/K)	$\lambda_{\text{exc}}/\text{nm}$	$\lambda_{\text{em}}/\text{nm}$	ϕ	τ
[NBu ₄] ₂ [Pt(C ₆ F ₅) ₄]	solid (77)	323	423, 440		
	CH ₂ Cl ₂ (77) ^a	311	432		
[(C ₆ F ₅) ₄ PtCd(cyclen)] (1)	solid (298, 77)		no emissive		
	CH ₂ Cl ₂ (77) ^b	320max, 342(λ_{em} 466) 320, 370max (λ_{em} 525)	444max, 487, 570 (λ_{ex} 340) 466max, 545(λ_{ex} 360) 473, 546max(λ_{ex} 370)		
[PMePh ₃] ₂ [Pt(C ₆ F ₅) ₂ (C≡CPh) ₂]	solid (298)	337, 362, 382, 392, 433	451		957.8 ns
	solid (77)	313, 341	444max, 464, 475, 489, 515		(74%, χ^2 1.10)
	CH ₂ Cl ₂ (77)	313, 324, 333	430max, 452, 471		
	acetone (77)	321, 335	437max, 459, 477		
[(C ₆ F ₅) ₂ (C≡CPh) ₂ PtCd(cyclen)] (2 ·2Me ₂ CO)	solid (298)	333, 339, 356, 408	451max, 468, 490 ^c		342.1 ns
	solid (77)	312, 340, 357, 407	446max, 469, 481, 492 ^c		(58%, χ^2 0.37)
	CH ₂ Cl ₂ (77)	326, 352, 400	445max, 479, 491, 517, 549 ^c		
	acetone (77)	315, 348	445max, 476, 510 ^c		
[NBu ₄][Pt(C ₆ F ₅) ₂ (bzq)] (6)	KBr (298)	334, 366, 392, 439, 480sh	524, 590sh		16.5 μ s
	solid (298)	344, 356, 391, 425sh, 432	518		
	solid (77)	334, 350, 394, 441, 478sh	514, 550, 595sh		
	acetone (298) ^a	380, 426max	486	0.0019 ^d	
	acetone (77)	365, 427	488, 526, 567, 611sh ^e		
	CH ₂ Cl ₂ (298)		no emissive		
	CH ₂ Cl ₂ (77)	328, 340, 389, 423	490, 525, 568		
[(C ₆ F ₅) ₂ (bzq)PtCd(cyclen)]ClO ₄ (3)	KBr (298)	356, 393, 407, 432, 479	488, 519, 560sh		7.9 μ s
	solid (298)	336, 392, 425	490, 518, 560sh		
	solid (77)	333, 396, 425	484, 518, 560sh		
	acetone (298)	380br, 432max	481	0.0285 ^d	
	acetone (77)	330, 358, 400	483, 517, 560sh		

^a Weak emission. ^b Saturated solution. ^c With tail to 600 nm. ^d Measured using dcm-pyram in MeOH as a standard. ^e With tail to 750 nm.

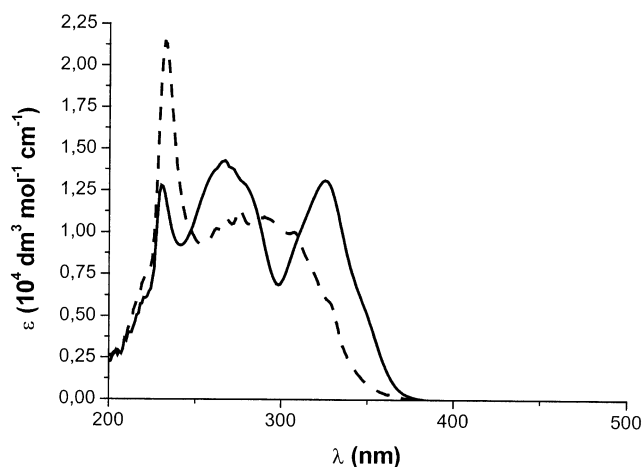


Figure 7. UV–visible spectra of [(C₆F₅)₂Pt(C≡CPh)₂Cd(cyclen)] (**2**) (—) and [PMePh₃]₂[Pt(C₆F₅)₂(C≡CPh)₂] (---) in CH₂Cl₂ solution (5 × 10⁻⁵ M).

CH₂Cl₂ solution (5 × 10⁻⁵ M) this band becomes resolved into three intense absorptions at 230, 267, and 325 nm with a small shoulder at 349 nm for **2**, while the precursor [PMePh₃]₂[Pt(C₆F₅)₂(C≡CPh)₂] exhibits in CH₂Cl₂ a high-energy band at 232 and a broad absorption profile with several maxima in the range 275–325 nm and a long tail to 360 nm (see Figure 7). Assignment is difficult because overlapping of π – π^* (IL, C₆F₅, C≡CPh) with bands due to PMePh₃⁺ is to be expected. The low-energy absorptions, which lie out of the range found in PMePh₃Br (<275 nm) and that are not observed in the homoleptic [NBu₄]₂[Pt(C₆F₅)₄] (236, 290 sh), can be tentatively ascribed, in both complexes, to an admixture of π → π^* (C≡CPh) IL/d π (Pt)– π^* (C≡CPh) MLCT. In fact, similar absorptions were found in the homoleptic derivative (NBu₄)₂[Pt(C≡CPh)₄]²¹ (335, 347 nm).

While the [NBu₄]₂[Pt(C₆F₅)₄] precursor exhibited a feeble luminescence structured band with maxima at 423 and 440 nm in the solid state at low temperature (77 K), probably due to an intraligand metal-perturbed ³($\pi\pi^*$) transition on the C₆F₅ rings (see Table 8 and Figure 2S in the Supporting Information), complex **1** is not emissive in the solid state. The absence of photoluminescence for **1** is not clear at this moment, but due to the formation of a Pt–Cd donor–acceptor bond in this complex, the Cd²⁺ behaves as a luminescence quencher only in the solid state. Both derivatives are nonemissive in fluid or frozen acetone solution. In frozen CH₂Cl₂ solution, the precursor [NBu₄]₂[Pt(C₆F₅)₄] also exhibits a weak emission at ca. 432 nm. The solubility of complex **1** in CH₂Cl₂ is very low. However, a frozen saturated CH₂Cl₂ solution displays a more complex behavior. Figure 8 shows the emission spectra, which are dependent on the excitation energy, thus indicating the existence of several emissive states. The low-energy emission (545 nm), which is absent in the precursor, is tentatively attributed to a transition related to the formation of the Pt–Cd bond.

The emission spectra of the precursor [PMePh₃]₂[Pt(C₆F₅)₂(C≡CPh)₂] in the solid state (at room temperature and 77 K and in frozen solutions (see Table 8)) show a structured band (444–430 nm) with progressional spacing suggestive of a combination of a vibrational mode of C≡C and Ph rings. With reference to earlier work on platinum(II)–alkynyl systems,^{2e,8j,21,22} the origin of the luminescence is assigned as derived from metal-perturbed triplet alkynyl intraligand states (π → π^* C≡CPh) mixed with some degree of metal-to-ligand (d π (Pt)→ π^* C≡CPh) charge transfer character.

(21) Benito, J.; Berenguer, J. R.; Forniés, J.; Gil, B.; Gómez, J.; Lalinde, E. *Dalton Trans.* **2003**, 4331.

(22) Fernández, S.; Forniés, J.; Gil, B.; Gómez, J.; Lalinde, E. *Dalton Trans.* **2003**, 822.

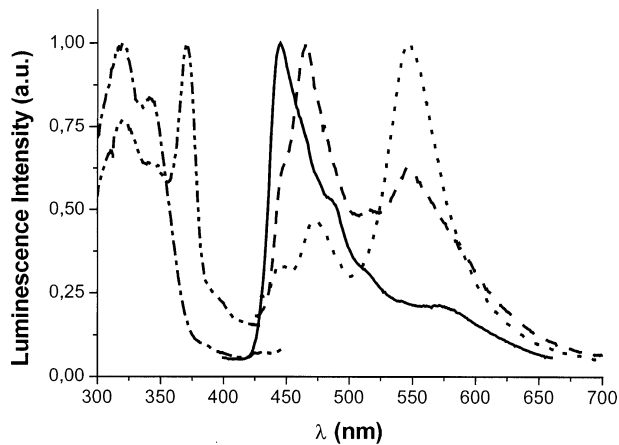


Figure 8. Excitation and emission spectra of $[(C_6F_5)_4PtCd(cyclen)]$ (**1**) in CH_2Cl_2 solution (77 K). Excitation: (—) λ_{ex} 340; (---) λ_{ex} 360; (···) λ_{ex} 370. Emission: (—) λ_{em} 525; (---) λ_{em} 466.

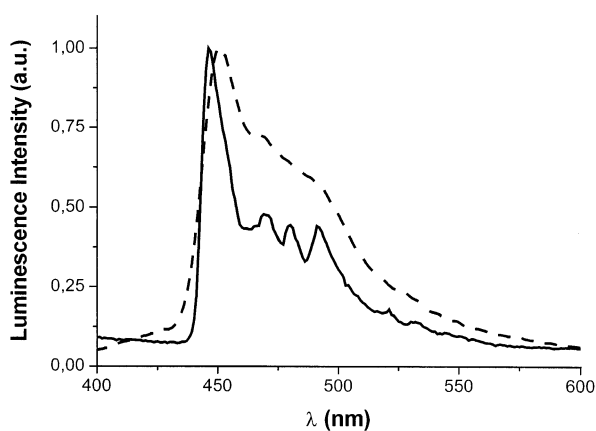


Figure 9. Emission spectra of $[(C_6F_5)_2Pt(C\equiv CPh)_2Cd(cyclen)]$ (**2**) in the solid state at 298 K (---) and at 77 K (—).

Curiously, when the microcrystalline solid of $[(C_6F_5)_2(C\equiv CPh)_2PtCd(cyclen)]$ **2** is inside the methanolic solution in which it is precipitated, it also displays at room temperature a visible blue luminescence upon exciting with 365 nm by means of a hand-held, dual-wavelength mercury UV lamp, but this luminescence is lost when the solid is dried. Emission is, however, detected for this solid at 77 K at ca. 446 nm with a rich vibronic structure (see Table 8). Crystallization of **2** from acetone/hexane causes the incorporation of acetone in the lattice (see Figure 1S in the Supporting Information) with again a visible blue luminescence for the solid at room temperature, the intensity of which is enhanced by lowering the temperature. Figure 9 shows the luminescence emission of this solid (**2**: $2Me_2CO$) at room temperature and at 77 K. The structured emission observed at 77 K (446 nm) with vibrational spacing of 1100, 1632, and 2097 cm^{-1} is again suggestive of the involvement of alkynyl ligands in the optical transition. At 298 K, the emission max is slightly red-shifted (451 nm) relative to that observed for the precursor $[PMePh_3]_2[Pt(C_6F_5)_2(C\equiv CPh)_2]$ (444 nm) with a lifetime of 342.1 ns, shorter than that measured for $[PMePh_3]_2[Pt(C_6F_5)_2(C\equiv CPh)_2]$ (957.8 ns) and indicative of the forbidden nature of the transition responsible for the radiative decay of the excited state. In fluid acetone or CH_2Cl_2 solutions, no emission is detected, but again intense structured

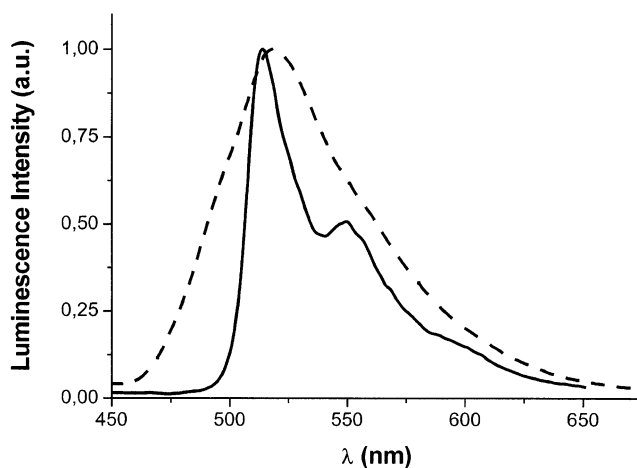


Figure 10. Emission spectra of $[NBu_4][Pt(C_6F_5)_2(bzq)]$ (**6**) in the solid state at 298 K (---) and at 77 K (—).

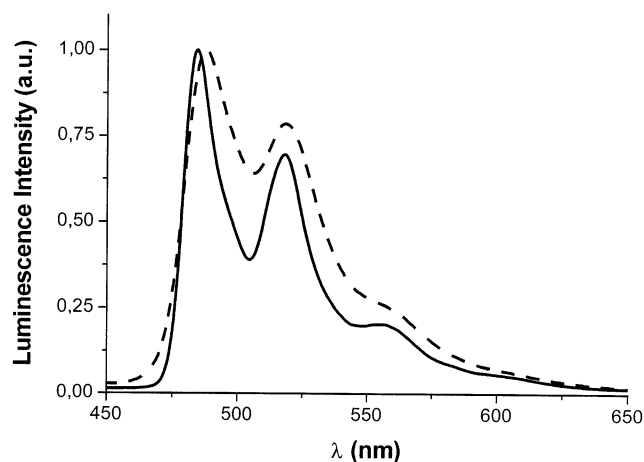


Figure 11. Emission spectra of $[(C_6F_5)_2(bzq)PtCd(cyclen)]-(ClO_4)$ (**3**) in the solid state at 298 K (---) and at 77 K (—).

features are observed upon cooling to 77 K. The emission maxima at 77 K (445 nm) are identical in both solvents, suggesting that the ${}^3IL(\pi-\pi^*C\equiv CPh)$ is more evident in the excited state of this complex at low temperature.

Like many cyclometalated platinum complexes, $[NBu_4][Pt(C_6F_5)_2(bzq)]$ (**6**) and the binuclear cationic $[(C_6F_5)_2(bzq)PtCd(cyclen)](ClO_4)$ (**3**) are emitters in both solution and in the solid state (see Table 8 and also Figures 10 and 11). While the room-temperature solid-state emission of **6** is relatively diffused, the 77 K emission is slightly blue-shifted and highly structured with C=C and C=N vibration modes of the bzq ligand (Figure 10). Similar structured, but blue-shifted, emissions are observed in frozen acetone or CH_2Cl_2 (10^{-5} – 10^{-3} M) solutions. In the solid state, the intrinsic lifetime (16.5 μ s), the emission, and the small hypochromic shift (298 K 518 nm; 77 K, 514 nm (max), 550, 595 (sh)) are similar to those reported for $[NBu_4][PtCl_2(bzq)]$ (298 K, 524 nm; 77 K, 514 (max), 554, 597 (sh))^{23c} and $[NBu_4][Pt(bzq)(C\equiv CR)_2]$ (508–533 nm).²² With reference to earlier work^{20,22,23} and the absence of any major solvatochromic shift we assign the emission as mixed ${}^3IL/{}^3MLCT$.

(23) (a) Brooks, J.; Babayan, Y.; Lamansky, S.; Djurovich, P. I.; Tsyba, I.; Bau, R.; Thompson, M. E. *Inorg. Chem.* **2002**, *41*, 3055. (b) Joliet, P.; Gianini, M.; von Zelewsky, A.; Bernardinelli, G.; Stoekli-Evans, H. *Inorg. Chem.* **1996**, *35*, 4883. (c) Lai, S. W.; Chan, M. C. W.; Cheung, K. K.; Peng, S. M.; Che, C. M. *Organometallics* **1999**, *18*, 3991.

In contrast to complex **6**, the emission spectrum of **3** is also vibrationally resolved even in the solid state at room temperature with peak maxima at 490 and 518 (560 sh), which are slightly blue-shifted at 77 K (see Figure 11). In fluid acetone solution, the emission is weak and unstructured with a maximum at 481 nm but again becomes highly structured in frozen solution (483, 517, 560 sh). On the basis of these observations, the emission is also assigned as ³MLCT transitions with ³-LC character. The substantial blue-shift (~1205 cm⁻¹) of the emission observed in the solid state for **3** in relation to that observed in the mononuclear precursor (77 K, 484 nm in **3** vs 514 nm in **6**) is consistent with the presence of the Pt→Cd donor–acceptor bond and in agreement with some degree of charge transfer for the transition. In this binuclear complex, the Cd²⁺ ion drains electron density from the platinum atom, making the transfer of charge away from the metal a more energetic process. The Pt→Cd bond seems to have also a marked effect on both the lifetime of the emission (7.9 μs in **3** vs 16.5 μs in **6**) and the luminescent efficiency (0.0285 in **3** vs 0.0019 in **6**; $K_r = 3.6 \times 10^3 \text{ s}^{-1}$ for **3**, $K_r = 0.115 \times 10^3 \text{ s}^{-1}$ for **6**).

Conclusions

Three novel binuclear Pt–Cd derivatives, **1–3**, stabilized by a short Pt→Cd donor acceptor bond have been synthesized. In the complex [(C₆F₅)₄PtCd(cyclen)] (**1**), the Pt–Cd distance is longer (2.775(1) Å) than those found in **2** and **3**, suggesting that the presence of bulky C₆F₅ ligands hinder the closing up of the basic Pt center to the acidic Cd metal. In fact, substitution of two C₆F₅ groups for a planar benzoquinolate ligand in complex **3** allows a better approach of the Cd center to the Pt center (Pt–Cd 2.688(1) Å), although one would expect lower basic behavior of the monoanionic [Pt(C₆F₅)₂(bzq)]⁻ fragment than of the dianionic one. On the other hand, in the complex [(C₆F₅)₂Pt(C≡CPh)₂Cd(cyclen)] (**2**) one of the phenylethynyl ligands of the dianionic entity [*cis*-Pt(C₆F₅)₂(C≡CPh)₂]²⁻ clearly competes with the platinum center to interact with the “[Cd(cyclen)]²⁺” moiety in such a way that in this complex the Cd center moves away from the normal to the platinum coordination plane, being bonded not only to Pt but also to the C_α atom of the acetylenic fragment. Finally, the use of the dinuclear substrate [NBu₄]₂[Pt₂(μ-Cl)₂(C₆F₅)₄] as a building precursor causes the asymmetric breaking of the bridging system and the final formation of the dimer [Pt(C₆F₅)₂Cl(μ-Cl)Cd(cyclen)]₂ (**4**) containing Cd–Cl bonds.

The optical properties of complexes **1–3** have also been described. However, the very different electronic nature of the platinum fragment used makes it, at the moment, very difficult to establish a clear relationship between the donor–acceptor Pt→Cd bond and the electronic excited states. Thus, it is somewhat surprising that the visible blue luminescence observed in the precursor [PMePh₃]₂[Pt(C₆F₅)₂(C≡CPh)₂] is clearly lost for the unsolvated Pt–Cd complex **2**, suggesting that [Cd(cyclen)]²⁺ acts a quencher. In the solid state at room temperature, the luminescence of this complex shows an interesting solvent dependence, which seems to be related to the existence of channels in the lattice. However, at low temperature (solid and frozen solution)

only typical structured emission bands associated with mixed ³MLCT(dπ(Pt)→π*(C≡CPh))/³IL(π→π*(C≡CPh)), and similar to those seen in the precursor, are observed. For complex **3**, the formation of the Pt–Cd bond clearly accounts for the substantial blue-shift in the observed emission in relation to that of the precursor **6** (solid 490 nm in **3** at 298 K vs 518 nm in **6**). The presence of the Pt→Cd acceptor bond probably stabilizes the HOMO, increasing the corresponding LUMO–HOMO energy gap and, hence, increasing the MLCT energy transition. It is remarkable that in both complexes **2** and **3** the formation of the Pt→Cd bond causes a significant decrease in the lifetime of the emission.

Experimental Section

General Comments. Literature methods were used to prepare the starting materials [NBu₄]₂[Pt(C₆F₅)₄],²⁴ [NBu₄]₂[Pd(C₆F₅)₄],²⁴ [NBu₄]₂[Pt(C₆Cl₅)₄],²⁴ [PMePh₃]₂[Pt(C₆F₅)₂(C≡CPh)₂],¹³ [NBu₄][Pt(C₆F₅)₃(bzq)],¹⁰ⁱ and [NBu₄]₂[Pt₂(μ-Cl)₂(C₆F₅)₄].^{24,25} Cyclen (1,4,7,10-tetraazacyclododecane) was commercially purchased (Aldrich) and used as delivered. C, H, and N analyses and mass, IR, and NMR spectra were performed as described elsewhere. Molar conductances were carried out on a Philips PW9509 conductimeter in acetone and dichloromethane solutions (5 × 10⁻⁴ M). The optical absorption spectra were recorded using a Hewlett-Packard 8453 (solution) spectrophotometer in the visible and near-UV ranges. Luminescence and excitation spectra were recorded using a Pekin-Elmer LS 50B luminescence spectrometer with an R928 type red sensitive photomultiplier and standard calibrated 1000 W xenon lamp (excitation). Emission lifetime measurements were performed in the frequency domain with a Fluorolog-3 model FL3-11 with F1-1029 lifetime emission PMT assembly, using a 450 W Xe lamp. The solution emission quantum yields were measured by the Demas and Crosby method,²⁶ using dcm-pyram [4-(dicyanomethylene)-2-methyl-6-(4-dimethylaminostyryl)-4H-pyrimidin-5(1H)-one] in degassed MeOH as the standard.

Safety Note: Perchlorate salts of metal complexes with organic ligands are potentially explosive. Only small amounts of material should be prepared, and these should be handled with great caution.

Synthesis of [Cd(cyclen)(MeOH)₂](ClO₄)₂. Cyclen (0.025 g, 0.146 mmol) was added to a MeOH (6 mL) solution of Cd(ClO₄)₂·6H₂O (0.068 g, 0.22 mmol). The initial suspension, which became a transparent solution after a few minutes, was refluxed for 1 h. The solution of the complex [Cd(cyclen)(MeOH)₂](ClO₄)₂ formed was allowed to reach room temperature and used in situ.

Synthesis of [(C₆F₅)₄PtCd(cyclen)] (1**).** [NBu₄]₂[Pt(C₆F₅)₄] (0.20 g, 0.146 mmol) was added to a MeOH (10 mL) solution of [Cd(cyclen)(MeOH)₂](ClO₄)₂ (0.146 mmol) prepared in situ. After a few minutes, the initial suspension became a transparent solution, from which a white solid precipitated after ~20 min of stirring. The suspension was stirred for 40 min more, and then the white solid was filtered off. This solid was washed with CHCl₃ (2 × 3 mL) and *n*-hexane (5 mL) and vacuum-dried (**1**, 56% yield). Anal. Calcd (%) for C₃₂H₂₀F₂₀N₄CdPt: C 33.45, H 1.76, N 4.87. Found: C 33.38, H 1.76, N 4.83. IR (Nujol): ν 773 cm⁻¹ (s; C₆F₅, X-sensitive vibr.).²⁷ Λ_M = 42 (acetone) Ω⁻¹ cm² mol⁻¹. ¹H NMR (HDA, rt): 3.24 (br, 4H, N–H), 3.07 (m, 8H), 2.91 ppm (m, 8H). ¹⁹F NMR (HDA, rt): –109.0 (d, 8F, *o*-F, $J_{\text{Pt-F}} = 526.9 \text{ Hz}$), –162.3 ppm (m, 12F,

(24) Usón, R.; Forniés, J.; Martínez, F.; Tomás, M. *J. Chem. Soc., Dalton Trans.* **1980**, 888.

(25) Usón, R.; Forniés, J.; Tomás, M.; Fandos, R. *J. Organomet. Chem.* **1984**, 263, 253.

(26) Demas, J. N. G.; Crosby, A. *J. Phys. Chem.* **1971**, 75, 991.

(27) Maslowsky, E., Jr. In *Vibrational Spectra of Organometallic Compounds*; Wiley: New York, 1977; p 437.

m-F + *p*-F). Crystals suitable for X-ray diffraction analysis were obtained by slow diffusion of a layer of *n*-hexane (20 mL) into a solution of **1** in 5 mL of Me₂CO at 4 °C.

Reaction of [NBu₄]₂[Pt(C₆Cl₅)₄] with [Cd(cyclen)(MeOH)₂](ClO₄)₂. [NBu₄]₂[Pt(C₆Cl₅)₄] (0.25 g, 0.146 mmol) was added to a MeOH (10 mL) solution of [Cd(cyclen)(MeOH)₂](ClO₄)₂ (0.146 mmol) prepared in situ. After 1 h of stirring the solution was evaporated to dryness. Treatment of the resulting white residue with ³PrOH (30 mL) produced a solid that was filtered and identified as the starting material [NBu₄]₂[Pt(C₆Cl₅)₄].

Reaction of [NBu₄]₂[Pd(C₆F₅)₄] with [Cd(cyclen)(MeOH)₂](ClO₄)₂. [NBu₄]₂[Pd(C₆F₅)₄] (0.18 g, 0.146 mmol) was added to a MeOH (10 mL) solution of [Cd(cyclen)(MeOH)₂](ClO₄)₂ (0.146 mmol) prepared in situ. After 1 h of stirring at room temperature the solution was evaporated to dryness. Treatment of the resulting white residue with ³PrOH (30 mL) produced a solid that was filtered and identified mostly as the starting material [NBu₄]₂[Pd(C₆F₅)₄], along with some small fractions of decomposition products, which we were not able to identify.

Synthesis of [(C₆F₅)₂(C≡CPh)₂PtCd(cyclen)] (2). To a white suspension of [PMePh₃]₂[Pt(C₆F₅)₂(C≡CPh)₂] (0.25 g, 0.194 mmol) in MeOH (60 mL) were added cyclen (0.033 g, 0.194 mmol) and CdClO₄·6H₂O (0.081 g, 0.194 mmol) to give a pale yellow solution. Immediately a very pale yellow solid started forming. After 15 min of stirring, the pale yellow solid was filtered (0.076 g). By evaporation to a small volume of the solvent (~10 mL) a second fraction was obtained (0.034 g) (44% yield). Anal. Calcd (%) for C₃₆H₃₀F₁₀N₄CdPt: C 42.55, H 2.98, N 5.51. Found: C 42.34, H 2.74, N 5.33; IR (Nujol): ν 2097 (vs), 2080 (sh) cm⁻¹ (C≡C); 766, 758 cm⁻¹ (s; C₆F₅, X-sensitive vibr.).²⁷ $\Lambda_M = 3.3$ (acetone) Ω^{-1} cm² mol⁻¹. ¹H NMR (HDA, rt): aromatics: 7.29 (m, 4H), 7.19 (m, 6H); cyclen ligand: 3.13 (br, 4H, N-H), 2.95 (m, 8H), 2.86 ppm (m, 8H). ¹⁹F NMR (HDA, rt): -116.0 (d, 4F, *o*-F, $J_{Pt-F} = 348.1$ Hz), -166.5 ppm (m, 6F, *p*-F + *m*-F); at 190 K: -115.5 (d, 1F, *o*-F, $J_{o-F-m-F} = 30$ Hz, $J_{Pt-F} = 422$ Hz), -116.0 (d, 1F, *o*-F, $J_{o-F-m-F} = 30$ Hz, $J_{Pt-F} \approx 315$ Hz), -116.3 (d, 1F, *o*-F, $J_{o-F-m-F} = 26$ Hz, $J_{Pt-F} \approx 315$ Hz), -117.5 (d, 1F, *o*-F, $J_{o-F-m-F} = 26$ Hz, $J_{Pt-F} = 420$ Hz), -165.86, -165.97, -166.0 ppm (2*p*-F + 4*m*-F). Crystals suitable for X-ray diffraction analysis were obtained by slow evaporation of a saturated solution of **2** in Me₂CO at 20 °C.

Synthesis of [NBu₄]₂[Pt(C₆F₅)₂(bzq)] (6). A 1,2-dichloroethane (20 mL) solution of [NBu₄]₂[Pt(C₆F₅)₂(bzq)] was refluxed for 3 h. After this time, the solution is allowed to reach room temperature and was evaporated to dryness and the orange residue treated with ³PrOH (10 mL) and filtered off, washed with *n*-hexane (5 mL), and vacuum-dried (63% yield). Anal. Calcd (%) for C₅₁H₃₆F₁₀N₄Pt: C 51.80, H 4.64, N 2.94. Found: C 51.14, H 4.07, N 2.83. IR (Nujol): ν 766, 796 cm⁻¹ (s; C₆F₅, X-sensitive vibr.).²⁷ ¹H NMR (HDA, rt): 7,8-benzoquinolate ligand: 7.80 (m, 6H), 8.50 (d, 1H), 8.67 (d, 1H) $J_{Pt-H} = 33.6$ Hz; NBu₄⁺ 1.00 (t, 12H, CH₃), 1.45 (q, 8H, γ -CH₂), 1.77 (m, 8H, β -CH₂), 3.45 (m, 8H, α -CH₂). ¹⁹F NMR (HDA, rt): -112.1 (d, 2F, *o*-F, $J_{Pt-F} = 360.6$ Hz), -112.4 (d, 2F, *o*-F, $J_{Pt-F} = 651.0$ Hz), -163.6 (m, 2F, *m*-F), -166.2 (m, 2F, *m*-F), -164.5 ppm (m, 1F, *p*-F), -167.2 (m, 1F, *p*-F).

Synthesis of [(C₆F₅)₂(bzq)PtCd(cyclen)](ClO₄) (3). [NBu₄]₂[Pt(C₆F₅)₂(bzq)] (0.083 g, 0.087 mmol) was added to a MeOH (8 mL) solution of [Cd(cyclen)(MeOH)₂](ClO₄)₂ (0.087 mmol) prepared in situ. After a few minutes, a yellow solid precipitated from the yellow solution. The resulting suspension was stirred for 1 h, and then the yellow solid was filtered off. This solid was washed with *n*-hexane (5 mL) and vacuum-dried (**3**, 50% yield). Anal. Calcd (%) for C₃₃H₂₈F₁₀N₅O₄ClCdPt: C 36.28, H 2.56, N 6.41. Found: C 36.11, H 2.39, N 6.39. IR (Nujol): ν 776, 801 cm⁻¹ (s; C₆F₅, X-sensitive vibr.).²⁷ $\Lambda_M = 81$ (acetone) Ω^{-1} cm² mol⁻¹. ¹H NMR (HDA, rt): 7,8-benzoquinolate ligand: 7.83 (m, 6H), 8.80 (d, 1H), 8.95 (d, 1H) $J_{Pt-H} = 23.7$ Hz; cyclen ligand: 2.26 (br, 4H, NH), 2.42 (m, 8H, CH₂), 2.57

(m, 8H, CH₂). ¹⁹F NMR (HDA, rt): -112.3 (d, 2F, *o*-F, $J_{Pt-F} = 407.0$ Hz), -115.1 (br, 2F), -162.5 (m, 1F, *p*-F), -163.3 (m, 2F, *m*-F), -163.7 ppm (m, 1F, *p*-F), -165.0 (m, 2F, *m*-F).

Synthesis of [Pt(C₆F₅)₂Cl₂Cd(cyclen)]₂ (4). [NBu₄]₂[Pt₂(μ -Cl)₂(C₆F₅)₄] (0.23 g, 0.146 mmol) was added to a MeOH (10 mL) solution of [Cd(cyclen)(MeOH)₂](ClO₄)₂ (0.146 mmol) prepared in situ. The resulting white suspension was stirred for 1 h, and then the white solid was filtered off. This solid was washed with CHCl₃ (2 × 3 mL) and *n*-hexane (5 mL) and vacuum-dried (**4**, 29% yield). Anal. Calcd (%) for C₄₀H₄₀F₂₀N₄Cl₄Cd₂Pt₂: C 27.13, H 2.26, N 6.33. Found: C 27.28, H 2.23, N 6.27. IR (Nujol): ν 810, 799 cm⁻¹ (s; C₆F₅, X-sensitive vibr.).²⁷ ¹H NMR (HDA, rt): 3.50 (br, 4H, N-H), 3.16 (m, 8H), 2.90 ppm (m, 8H). ¹⁹F NMR (HDA, rt): -115.2 (d, 8F, *o*-F, $J_{Pt-F} = 528.2$ Hz), -162.1 ppm (m, 4F, *p*-F), -163.0 ppm (m, 8F, *m*-F). Crystals suitable for X-ray diffraction analysis were obtained by slow diffusion of a layer of *n*-hexane (20 mL) into a solution of 25 mg of **4** in 5 mL of Me₂CO at 4 °C.

Synthesis of [Cd₂(μ -Cl)₂(cyclen)₂](ClO₄)₂ (5). (NBu₄)Cl (0.08 g, 0.290 mmol) was added to a MeOH (10 mL) solution of [Cd(cyclen)(MeOH)₂](ClO₄)₂ (0.290 mmol) prepared in situ, and the precipitation of a white solid is observed almost immediately. This white solid was filtered off and vacuum-dried (**5**, 52% yield). Anal. Calcd (%) for C₁₆H₄₀Cl₄N₈O₈Cd₂: C 22.88, H 4.77, N 13.25. Found: C 23.33, H 5.32, N 13.50. ¹H NMR (DMSO, rt): 2.62 (br, 4H, N-H), 2.49 (m, 16H).

X-ray Structure Determinations. Crystal data and other details of the structure analyses are presented in Table 1. Crystals were mounted at the end of a quartz fiber. The radiation used in all cases was graphite-monochromated Mo K α ($\lambda = 0.71073$ Å).

For **1**·2Me₂CO, **3**·0.5MeOH, **4**·2Me₂CO, and **5**, hemispheres of X-ray intensity data were collected on a Bruker SMART APEX diffractometer. An absorption correction was applied on the basis of 3219, 4477, 3132, and 1696 symmetry equivalent reflection intensities, respectively. For **2**·2Me₂CO, X-ray intensity data were collected with a NONIUS κ CCD area-detector diffractometer. Images were processed using the DENZO and SCALEPACK suite of programs.²⁸ The absorption correction was performed using SORTAV.²⁹

The structures, except **2**·2Me₂CO, were solved by Patterson and Fourier methods using the program SHELXS-97.³⁰ The structure of **2**·2Me₂CO was solved using the DIRDIF92³¹ program. The structures were refined by full-matrix least squares on F^2 with SHELXL-97. All non-hydrogen atoms were assigned anisotropic displacement parameters and refined without positional constraints except as noted below. All hydrogen atoms were constrained to idealized geometries and assigned isotropic displacement parameters equal to 1.2 times the U_{iso} values of their attached parent atoms (1.5 times that for the methyl hydrogen atoms). In the structure of **2**·2Me₂CO, two molecules of the crystallization solvent were found in the asymmetric unit. One of the acetone molecules was found to be disordered, and to model this molecule, the O(100)–C(90) distance was constrained to 1.2(0.01) Å, while the methyl carbon atoms (C(92), C(91)) were constrained to a distance of 1.50(0.01) of the carbonyl carbon atom C(90). In the structure of **3**·0.5MeOH, a molecule of MeOH, one of the solvent molecules used for the preparation of the complex, was found and refined with partial occupancy of 0.5. The OH hydrogen atom of the methanol moiety was not added to the model. In the structures of **2**·2Me₂CO, **4**·2Me₂CO, and **5**, the

(28) Otwinowski Z.; Minor, W. *Methods Enzymol. A: Macromol. Crystallogr.* **1997**, 276, 307.

(29) Blessing, R. H. *Acta Crystallogr., Sect. A* **1995**, 51, 33.

(30) Sheldrick, G. M. *SHELX-97*, a program for the refinement of crystal structures; University of Göttingen, Germany, 1997.

(31) Beursken, P. T.; Beursken, G.; Bosman, W. P.; de Gelsel, R.; Garcia Granda, S.; Gould, R. O.; Smith J. M. M.; Smykalla, C. *The DIRDIF92 program system*, Technical Report of the Crystallography Laboratory; 1992.

cyclen ring was found to be disordered over two positions. The disordered sets of atoms were refined with partial occupancy of 0.70/0.30 for **2**·2Me₂CO, 0.75/0.25 for **4**·2Me₂CO, and 0.50/0.50 for **5**. For **2**·2Me₂CO, common sets of thermal anisotropic parameters were used for the nitrogen atoms and for the carbon atoms of the minor component of the disorder. For **4**·2Me₂CO, C–C and C–N distances were constrained to sensible values and common sets of thermal anisotropic parameters were used for the nitrogen atoms of both components and the carbon atoms of the minor component of the disorder. For **5**, the C–C and C–N distances were restrained to be equal. Full-matrix least-squares refinement of these models against F^2 converged to final residual indices given in Table 1.

Acknowledgment. Financial support has been obtained from the Ministerio de Ciencia y Tecnología and

FEDER (Project BQU2002-03997-C02-01, 02), the Diputación General de Aragón (Grupos Consolidados), and the Comunidad de La Rioja (ACPI-2002/08). S.I. and B.G. thank the Ministerio de Ciencia y Tecnología and the CSIC, respectively, for a grant.

Supporting Information Available: Listings of atomic coordinates, bond distances and angles, and thermal parameters for **1**·2Me₂CO, **2**·2Me₂CO, **3**·0.5MeOH, **4**·2Me₂CO, and **5**. Extended structure of [(C₆F₅)₂Pt(C≡CPh)₂Cd(cyclen)]·2CH₃COCH₃ (**2**·2CH₃COCH₃) (Figure 1S) and excitation and emission spectra of [NBu₄]₂[Pt(C₆F₅)₄] in the solid state at 77 K (Figure 2S). This material is available free of charge via the Internet at <http://pubs.acs.org>.

OM049719W